

Pontificia Universidad Católica del Perú
Escuela de Posgrado



**Self Image and Simulation of a PR-box
using High-order paraxial beams**

A thesis in candidacy for the degree of Master of
Science in Physics

Presented by
Victor Andre Avalos Pinillos

Advisors
Francisco Antonio de Zela Martinez (PUCP)
Antonio Zelaquett Khoury (UFF)

Lima-Perú-2019

Abstract

From Maxwell equations (for a free of charge and current, isotropic and homogeneous medium) and the paraxial approximation, which is to suppose the beam of light moves towards a preferred direction (longitudinal propagation), we arrive at the paraxial wave equation, which depending of the constraints of the situation, can be solved by different type of beams. We are interested in higher-order mode paraxial beams. If we solve the equation with cartesian coordinates, we arrive at Hermite-Gauss beams, if we solve with cylindrical coordinates, we obtain Laguerre-Gauss beams. Each of them has specific characteristics which motivated their use in the two phenomenons presented here: Self Image and the Simulation of a PR box.

We call self image to the phenomenon where we are capable of replicating an initial image, over free space longitudinal propagation. What we propose here is a self image produced by the collinear and coherent interference of paraxial Laguerre Gauss (LG) beams, which contrasts with the usage of a fundamental Gaussain beam in Talbot's self image. Gouy phases, which are the key component that make this phenomenon possible, are exclusive of Higher-order paraxial beams. We show, experimentally, the phenomenon of self image using the superposition of 3 LG beams with specific mode orders. Because of the arctangent dependence of the Gouy phases, in Laguerre-Gaussian beams, self image distances won't be periodic over propagation and its number will be limited by the mode orders of the LG beams. Additionally, we use this superposition of the 3 LG beams as dots, to write a word, which can be read only in self image. This application of self image can be thought of as concealing information, and then revealing it only for specific distances.

The most controversial feature of quantum mechanics non-locality, has gain much attention over the last years, because of the development of quantum information. Nowadays non-locality is widely accepted and used in many other exciting applications like teleportation, swapping, etc. Nevertheless, this opens other questions, like why is nature just as non-local as to reach the Tsirelson's bound, but can't surpass it. The algebraical maximum of the CHSH inequality is 4, and quantum mechanics can only reach up to $2\sqrt{2}$. What happens in this gap that seems empty and without a theory that can describe it? In 1993, Popescu and Rhorlich proved that from non-locality and relativistic causality, quantum

mechanics was not the only theory that emerged. Relativistic causality, meaning that no information is transmitted with superluminal velocities. This means that there are super-quantum correlations, that surpass the Tsirelson's bound, and are still causal. The super-quantum correlations that maximally surpass the Tsirelson's bound, making the Bell parameter $S = 4$, are known as PR boxes. Markovitch et al, showed that, in a bipartite quantum system, post-selecting an entangled state will fake the maximal surpass of the Tsirelson's bound in the Bell inequality. Here, we propose an experimental setup capable of simulating a PR box using polarization and transverse-mode (Hermitian-Gauss beams of first order) of light as vector spaces that are analogue to Hilbert spaces in quantum mechanics.



Acknowledgments

This thesis is the result of the work I did during my stay of 4 months in the Quantum Optics Group at the Universidad Federal Fluminense, there I had the privilege to be under the guidance of Prof. Zelaquett to whom I thank for receiving me and taking the time to explain and discuss many concepts and ideas with me. I would also like to thank Braian with whom I worked during the most part of my stay. And also to everyone in the group for making my experience in Niterói a lot more pleasant than I could anticipate.

Also, none of this could have been possible without what I learned in the Quantum Optics Group at PUCP. I would like to thank Prof. de Zela for opening the doors of this group to many enthusiasts of Quantum Mechanics as me, and sharing with us his insight. Also I want to thank everyone at the group, for making the experimental work more enjoyable and for all the discussions from where I rescue many things that I believe have made me a better researcher.

I want to thank my family for encouraging me and giving me their support through all this journey.

Finally, thanks to CONCYTEC for the scholarship that vanished any worry about money for the duration of the Master degree program and let me focus entirely on the development of this thesis.

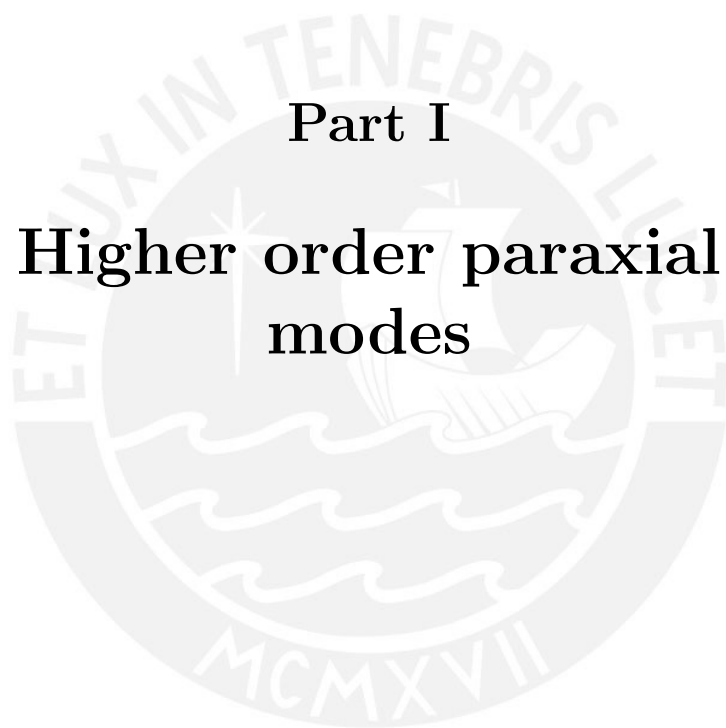
Contents

I	Higher order paraxial modes	8
1	Paraxial equation of light	9
1.1	Solutions to the paraxial wave equation	10
1.1.1	Fundamental Gauss mode	10
1.1.2	Hermite-Gauss mode	11
1.1.3	Laguerre-Gauss mode	11
II	Self image	12
2	Introduction: Self image	13
3	Ray matrices or ABCD matrices	14
3.1	Telescope	15
3.2	Longitudinal displacement	16
4	Propagation of a paraxial LG beam through z	17
4.1	Behavior of $A_{p,l}(r, z)$ when the beam propagates through z	18
4.2	Interference of various Laguerre-Gauss beams	19
4.3	Self image with paraxial LG beams	19
4.3.1	Self image with 2 LG beams	22
4.3.2	Self image with 3 LG beams	22
4.3.3	Example	23
5	Application: Concealing information using the superposition of LG beams	25
5.1	Using superposition of LG beams to write a word	25
5.2	Spatial Light Modulator: generation of the superposition of LG beams	25
5.3	Experimental setup	26
5.4	Experimental results	28
6	Conclusions	30

III	PR box	31
7	Introduction: PR box	32
8	PR box: Non-locality beyond quantum mechanics	34
8.1	Non-locality	34
8.2	Entanglement and Non-locality	34
8.3	CHSH inequality	35
8.4	Axioms of Quantum Mechanics	36
8.5	Black Box	36
8.6	CHSH inequality: revisited	37
8.7	PR box	38
8.8	CHSH inequality: PR box	38
8.9	PR-boxes in Communication Complexity	39
9	Simulation of a PR-box using a Quantum Mechanics ensemble	41
9.1	Measurements in Quantum Mechanics	41
9.2	The Aharonov-Bergman-Lebowitz formula	42
9.3	With what quantum pre and post selected states can we simulate a PR box?	43
10	Experimental Proposal to simulate a PR-box using polarization and transverse mode spaces	45
10.1	Polarization and transverse mode as vector spaces	45
10.2	Local Unitary Operations	46
10.2.1	Local Unitary operators in polarization space	46
10.2.2	Local Unitary operators in transverse-mode space	47
10.3	Projectors	48
10.3.1	Polarizing beam splitter	48
10.3.2	Transverse-mode beam splitter	49
10.4	Stages to simulate a PR box	52
10.5	Proposed Experimental Setup	52
10.5.1	Pre-selection	53
10.5.2	Projective Measurements	54
10.5.3	Post-selection	56
10.5.4	Measurement of the probability distribution	59
11	Discussions	60
11.1	PR boxes make bits share too much information	60
11.2	Loopholes in Bell inequalities	61
11.3	Opinion on the application of PR-boxes in Communication Complexity	61
12	Conclusions	62

13 Annex	63
13.1 Jones matrix representation in the tripartite space	63
13.1.1 Half wave plate's	63
13.1.2 Mirror's	63
13.1.3 Beam Splitter's	63
13.2 Local unitary operations in a Bell state	63
13.3 Projections in a Bell state	65





Part I

**Higher order paraxial
modes**

Chapter 1

Paraxial equation of light

The Maxwell equations of light give us its dynamical behaviour, if we consider an homogeneous, isotropic and charge/current free medium, they become:

$$\vec{\nabla} \cdot \vec{E}(\vec{r}, t) = 0 \quad (1.1)$$

$$\vec{\nabla} \times \vec{E}(\vec{r}, t) = -\frac{\partial \vec{B}(\vec{r}, t)}{\partial t} \quad (1.2)$$

$$\vec{\nabla} \cdot \vec{B}(\vec{r}, t) = 0 \quad (1.3)$$

$$\vec{\nabla} \times \vec{B}(\vec{r}, t) = \frac{1}{c^2} \frac{\partial \vec{E}(\vec{r}, t)}{\partial t} \quad (1.4)$$

Having in mind that $\vec{\nabla} \times \vec{\nabla} \times \vec{E} = \vec{\nabla}(\vec{\nabla} \cdot \vec{E}) - \nabla^2 \vec{E} = -\nabla^2 \vec{E}$, where we used equation 1.1. This can be equaled to the rotational of equation 1.2, and also using 1.4, we obtain:

$$\vec{\nabla}^2 \vec{E}(\vec{r}, t) = \frac{\partial \vec{\nabla} \times \vec{B}(\vec{r}, t)}{\partial t} = \frac{1}{c^2} \frac{\partial \vec{E}(\vec{r}, t)}{\partial t} \quad (1.5)$$

an analogous equation can be achieved for the magnetic field, so in resume we have:

$$\vec{\nabla}^2 \vec{E}(\vec{r}, t) = \frac{1}{c^2} \frac{\partial \vec{E}(\vec{r}, t)}{\partial t} \quad (1.6)$$

$$\vec{\nabla}^2 \vec{B}(\vec{r}, t) = \frac{1}{c^2} \frac{\partial \vec{B}(\vec{r}, t)}{\partial t} \quad (1.7)$$

From now on, we will only analyze the electric field 1.6. Because of the willing to describe a monochromatic beam propagating through a unique direction (let's assume it is the z direction), a solution can be pictured as:

$$\vec{E} = U(\vec{r}) e^{i(kz - \omega t)} \hat{\epsilon} \quad (1.8)$$

where $\hat{\epsilon}$ is the polarization vector, k is the wave number and $U(\vec{r}) e^{i(kz - \omega t)}$ is the wave amplitude. Notice, we are assuming the temporal dependence appears

only in the phase of the amplitude.

Using the solution 1.8 in 1.6, we obtain the Helmholtz equation:

$$\vec{\nabla}^2 U(\vec{r}) + 2ik\hat{z} \cdot \vec{\nabla} U(\vec{r}) = 0 \quad (1.9)$$

where \hat{z} is the unitary vector in the z direction. Again, the paraxial approximation is needed here because we are assuming a beam that propagates through a single direction and its transverse section doesn't change over this direction.

Mathematically, the paraxial approximation is as follows:

$$\frac{\partial^2 U}{\partial z^2} \ll \frac{\partial^2 U}{\partial x^2} + \frac{\partial^2 U}{\partial y^2} + 2k \frac{\partial U}{\partial z} \quad (1.10)$$

Using the paraxial approximation (1.10) in 1.9:

$$\vec{\nabla}_{\perp}^2 U(\vec{r}) + 2ik \frac{\partial U(\vec{r})}{\partial z} = 0 \quad (1.11)$$

where $\vec{\nabla}_{\perp}^2 = \frac{\partial^2}{\partial x^2} + \frac{\partial^2}{\partial y^2}$. This equation is known as the paraxial wave equation.

1.1 Solutions to the paraxial wave equation

1.1.1 Fundamental Gauss mode

The paraxial equation (1.11) admits many solutions [1], the one of less order is known as the fundamental Gauss mode:

$$u(r) = \sqrt{\frac{2}{\pi}} \frac{1}{w_z} \exp \left[-\frac{r^2}{w_z^2} + ik \frac{r^2}{2R_z} - i \arctan(z/z_r) \right] \quad (1.12)$$

where z_r is the Rayleigh distance:

$$z_r = \frac{\pi w_0^2}{\lambda} \quad (1.13)$$

where w_0 is the beam waist.

R_z is the curvature radius of the beam:

$$R_z = z \left(1 + \frac{z_r^2}{z^2} \right) \quad (1.14)$$

and w_z is the beam diameter over propagation through z .

$$w_z = w_0 \sqrt{1 + \frac{z_r^2}{z^2}} \quad (1.15)$$

Notice that the beam is characterized solely by w_0 and λ through the whole propagation.

1.1.2 Hermite-Gauss mode

If the paraxial equation is solved with rectangular coordinates, the solution is the Hermite Gauss modes :

$$HG_{(n,m)}(x, y, z) = \frac{B_{mn}}{w_z} e^{-\frac{r^2}{w_z^2}} H_n \left(\sqrt{2} \frac{x}{w_z} \right) H_m \left(\sqrt{2} \frac{y}{w_z} \right) \exp \left[-i \left(k \frac{r^2}{2R_z} \right) \right] e^{i\phi_N(z)} \quad (1.16)$$

where $B_{m,n} = \sqrt{\frac{2}{\pi m! n! 2^{n+m}}}$ is a normalization constant. H_m and H_n are the Hermite polynomials. $\phi_N = N \arctan(z/z_r)$ is the Gouy phase. $N = (n + m + 1)/2$ is by definition the mode order. In Figure 1.1 we show the intensity distribution images for different values of n and m .

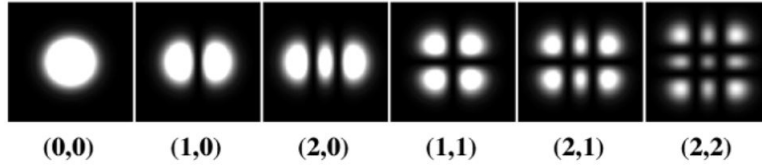


Figure 1.1: Intensity profile for different $HG_{(n,m)}$ modes.

1.1.3 Laguerre-Gauss mode

If the paraxial equation is solved in cylindrical coordinates, the solution is called Laguerre-Gauss mode, with orbital and radial orders l and p respectively, is:

$$LG_{(p,l)}(r, \theta, z) = \frac{C_{lp}}{w_z} \exp \left[-\frac{r^2}{w_z^2} - ik \left(\frac{r^2}{2R_z} + z \right) \right] L_{|l|,p} (2r^2/w_z^2) e^{-il\theta} e^{i\phi_N(z)} \quad (1.17)$$

Where, having in mind that w_0 is the beam's waist, $C_{lp} = \sqrt{\frac{2p!}{\pi(p+|l|)}}$ is a normalization constant, $L_{|l|,p} (2r^2/w_z^2)$ is the Laguerre polynomial with orders $|l|$ and p evaluated in $2(\frac{r}{w_z})^2$, $\phi_N(z) = (N+1) \arctan(\frac{z}{z_r})$ is known as Gouy phase, where $N = 2p + |l|$ is the mode order. The parameter p is known as radial charge and determines the number of rings in the transversal mode. The parameter l is called orbital charge, it determines the size of the rings. See Figure 1.2

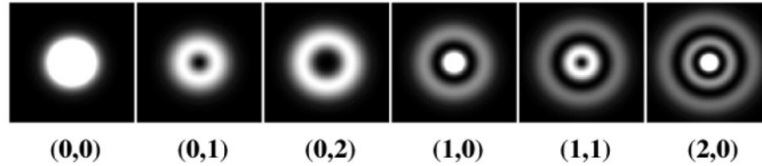


Figure 1.2: Intensity profile for different $LG_{(p,l)}$ modes.



Part II

Self image

Chapter 2

Introduction: Self image

Self image is the phenomenon where we are capable of replicating an initial image, over free space longitudinal propagation of a beam of light.

The concept's history goes back to 1836 when William Fox Talbot discovered that when a periodic diffracting grating was illuminated with a plane wave, the image of the grating was repeated periodically. This effect appears when using plane waves and fundamental gaussian modes of light. What we propose here is self image using the superposition of various collinear paraxial Laguerre Gauss beams with different mode orders.

In chapter 3, we review the ABCD matrices to represent different medium setups made of lenses that will be useful for manipulating the LG beams. In chapter 4 we study the propagation of a single Laguerre Gauss (LG) beam and what happens with the intensity distribution (image) of the transverse section compared to the initial one. With this result, we analyze the image obtained from the superposition of various LG beams through propagation. Then we find what condition the various LG beams need to obey so that self image would be possible. In chapter 5 we show an experimental application of the LG beam's self image phenomenon: the revealing or concealing of information depending on the distance the beams propagated.

Chapter 3

Ray matrices or ABCD matrices

In order to describe the propagation of paraxial optical beams through homogeneous optical media, we define matrices that help us predict its effect on the beam's parameters. For this purpose, we characterize a ray (paraxial beam) with its displacement from the axis r and its slope $r' = dr/dz$ as in Figure 3.1. Since we are gonna deal with paraxial beams, θ will be really small and we can make the approximation $\tan \theta \cong \theta$, so the slope is $r' = \theta$. Let's call r_1 and r'_1 (r_2 and r'_2) to the coordinates of the incident (output) ray to the media [2].

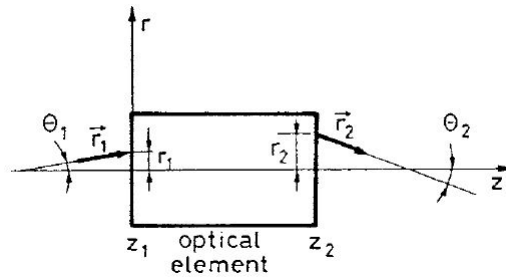


Figure 3.1: Propagation of a ray through a general optical element

Then, the effect of the optical media can be described as:

$$r_2 = A r_1 + B r'_1 \quad (3.1)$$

$$r'_2 = C r_1 + D r'_1 \quad (3.2)$$

which can be summarized as:

$$\begin{pmatrix} r_2 \\ r'_2 \end{pmatrix} = M \begin{pmatrix} r_1 \\ r'_1 \end{pmatrix} \quad (3.3)$$

where $M = \begin{pmatrix} A & B \\ C & D \end{pmatrix}$ is the ABCD matrix, which represents the effect of the optical homogeneous media on the optical ray.

If the optical media is a thin lens with focal length f , it is known that the ABCD matrix is:

$$M_{lens} = \begin{pmatrix} 1 & 0 \\ -1/f & 1 \end{pmatrix} \quad (3.4)$$

where $f > 0$ for a converging lens and is negative for a diverging one. From now on, we would suppose that $f > 0$ because we are interested only in converging lenses.

In the same way, we define the ABCD matrix of free media propagation:

$$M_{free} = \begin{pmatrix} 1 & d \\ 0 & 1 \end{pmatrix} \quad (3.5)$$

Now, if we want the ABCD matrix of a propagation through free media followed by a thin lens with focal distance f , we have to multiply both ABCD matrices:

$$M_+ = \begin{pmatrix} 1 & 0 \\ -1/f & 1 \end{pmatrix} \begin{pmatrix} 1 & d \\ 0 & 1 \end{pmatrix} \quad (3.6)$$

$$= \begin{pmatrix} 1 & d \\ -1/f & (1 - d/f) \end{pmatrix} \quad (3.7)$$

So as to obtain the ABCD matrix for a sequence of medias, we have to multiply their individual matrices, beginning from the right with the first media where the ray arrives.

3.1 Telescope

If we arrange two thin lenses with focal lengths f_1 and f_2 and a distance between them of $d = f_1 + f_2$, we can reduce or augment the transverse section of the beam. This is why this configuration is known as telescope. We used the telescope to collimate our beam.

The ABCD matrix of the telescope is:

$$\begin{aligned} M_{tel} &= M_{f_1} M_d M_{f_2} \\ &= \begin{pmatrix} 1 & 0 \\ -1/f_1 & 1 \end{pmatrix} \begin{pmatrix} 1 & f_1 + f_2 \\ 0 & 1 \end{pmatrix} \begin{pmatrix} 1 & 0 \\ -1/f_2 & 1 \end{pmatrix} \\ &= \begin{pmatrix} -f_1/f_2 & f_1 + f_2 \\ 0 & -f_2/f_1 \end{pmatrix} \end{aligned} \quad (3.8)$$

Something important for the telescope to work is that the incident beam has to be a paraxial beam propagating through the z axis. This will mean that the

slope r'_{in} is zero. So when we apply the telescope matrix on the incident beam's vector:

$$\begin{aligned} \begin{pmatrix} r_2 \\ r'_2 \end{pmatrix} &= M_{tel} \begin{pmatrix} r_1 \\ 0 \end{pmatrix} \\ &= \begin{pmatrix} -f_1 r_0 / f_2 \\ 0 \end{pmatrix} \end{aligned} \quad (3.9)$$

So we control the augmentation of the transverse section, with the relation of the focal lengths of the thin lenses:

$$r_2 = -\frac{f_1}{f_2} r_{in} \quad (3.10)$$

3.2 Longitudinal displacement

We can also displace the transverse section of the beam a certain distance (dependent of the focal lengths used)

The display is as follows. First, we have a free space propagation through a distance d_2 , then a thin lens with focal length $f_3 = d_2$. Thirdly, another free space propagation of distance $d_3 = 2f_3$. In addition a thin lens with focal length $f_4 = f_3$. Finally an additional free space propagation of length $d_4 = f_3$.

The ABCD matrix of the longitudinal displacement is:

$$\begin{pmatrix} r_2 \\ r'_2 \end{pmatrix} = M_{d_2} M_{f_3} M_{d_3} M_{f_4} M_{d_4} \begin{pmatrix} r_1 \\ r'_1 \end{pmatrix} \quad (3.11)$$

$$= \begin{pmatrix} -1 & 0 \\ 0 & -1 \end{pmatrix} \begin{pmatrix} r_1 \\ r'_1 \end{pmatrix} \quad (3.12)$$

$$= -\begin{pmatrix} r_1 \\ r'_1 \end{pmatrix} \quad (3.13)$$

This means from that point ($d = 4f_3$) forward, we have the same beam's transverse section propagation that we could have had right after the initial point ($d = 0$). This is why we call this configuration, longitudinal displacement.

Chapter 4

Propagation of a paraxial LG beam through z

We are interested in the superposition of various paraxial Laguerre beams through propagation. Let's initiate by analyzing a single paraxial LG beam.

We can rearrange the previous LG beam equation (1.17) according to our convenience:

$$LG_{(p,l)}(r, \theta, z) = e^{-i\alpha(r,z)} A_{p,l}(r, z) e^{-il\theta} e^{i\phi(z)} \quad (4.1)$$

Where the absolute value $A_{p,l}(r, z)$ is:

$$A_{p,l}(r, z) = \frac{C_{lp}}{w_z} \left(\sqrt{2} \frac{r}{w_z}\right)^{|l|} e^{-\left(\frac{r}{w_z}\right)^2} L\left(|l|, p, 2\left(\frac{r}{w_z}\right)^2\right) \quad (4.2)$$

In the equation (4.1) we have divided the Laguerre-Gauss expression in 4 components, we differentiate them because of their behaviour over the propagation across the z coordinate.

The first component $e^{-i\alpha(r,z)}$ won't be relevant in the analysis. Remember that we are interested in the superposition of various Laguerre beams. This component doesn't have dependence on the radial nor the orbital modes (l and p). So, through propagation, this component will be the same for all the LG beams.

The second component $A_{p,l}(r, z)$ is the absolute value of the expression. With an specific rescaling of the radial coordinate, that will be shown in the next section, we can demonstrate that this component contributes with an amplification of the image while the beam propagates.

The third component $e^{-il\theta}$ is the only one dependent on the azimuthal coordinate θ , since it doesn't depend on z , it won't change over the propagation. It will be different between LG beams only if their orbital mode l is different.

The fourth component $e^{i\phi(z)}$ is the one of most interest, where as stated before $\phi(z) = N \arctan(z/z_r)$ is known as the Gouy phase. If between two Laguerre beams, the mode order $N = 2p + |l| + 1$ of each of them is different ($N_1 \neq N_2$), then the Gouy phase will vary differently in each of them. But because of the periodic behaviour of $e^{i\phi(z)}$ it can be anticipated that gouy phases for the both beams can coincide for certain values of z .

4.1 Behavior of $A_{p,l}(r, z)$ when the beam propagates through z

As we can see in equation 4.2, $A_{p,l}(r, z)$ has a strong dependence on the term $\frac{r}{w_z}$, having this in mind we can do a change of coordinate:

$$\frac{r}{w_z} = \frac{r'}{w_0} \quad (4.3)$$

, where $w_0 = w_z(z = 0)$ and r' is a different value of the radial coordinate. Using (4.3), we can derive a new expression for the absolute value $A_{p,l}(r, z)$:

$$A_{p,l}(r, z) = \frac{C_{lp}}{w_z} (\sqrt{2} \frac{r'}{w_0})^{|l|} e^{-(\frac{r'}{w_0})^2} L\left(|l|, p, 2\left(\frac{r'}{w_0}\right)^2\right) \quad (4.4)$$

$$= \frac{w_0}{w_z} A_{p,l}(r', 0) \quad (4.5)$$

This means that the image in a different z position is the same as in the $z=0$ position, just with a different radial scaling ($\frac{r}{w_z} = \frac{r'}{w_0}$) which depends on the position z ($w_z = w_z(z)$).

Now we rewrite equation 1.17 using 4.5:

$$LG_{p,l}(r, \theta, z) = \frac{w_0}{w_z} e^{-i\alpha(r,z)} A_{p,l}(r', 0) e^{-il\theta} e^{i\phi(z)} \quad (4.6)$$

$$= \frac{w_0}{w_z} e^{-i(\alpha(r,z) - \alpha(r',0))} e^{i\phi_N(z)} LG_{p,l}(r', \theta, 0) \quad (4.7)$$

If we calculate the intensity distribution of the Laguerre beam at position z , using equation 4.7 we will get:

$$I(r, \theta, z) = \left(\frac{w_0}{w_z}\right)^2 I(r', \theta, 0) \quad (4.8)$$

This means the image, in the transverse section, that we see as the beam propagates through the z coordinate will be a magnification, in the radial direction, of the original image ($z=0$). Additionally the proportionality value $\left(\frac{w_0}{w_z}\right)^2$ tells us that, while the beam propagates it also loses intensity uniformly in the transverse section (independent of r or θ).

4.2 Interference of various Laguerre-Gauss beams

In the previous section we analysed the propagation of a single Laguerre-Gauss beam through the z direction. Nevertheless, of much more interest is the propagation of the superposition of 2 or more Laguerre-Gauss beams.

The expression for the superposition of q colinear Laguerre Gaussian beams is:

$$\begin{aligned} u_{sup}(r, \theta, z) &= LG_1(r, \theta, z) + LG_2(r, \theta, z) + \dots + LG_q(r, \theta, z) \quad (4.9) \\ &= \sum_i^q LG_i(r, \theta, z) \quad (4.10) \end{aligned}$$

where $LG_i = LG_{p_i, l_i}$.

The equation 4.10 showcases that all the beams are colinear and are originated at the same position, so all have the same coordinates r , θ and z . Also, all of them have the same beam waist w_0 and the same wavelength λ . So the only thing really differentiating them are the modes l and p (orbital and radial modes respectively). For the beam LG_i we will denote the orbital and radial modes as l_i and p_i respectively.

Using equation 4.7 in 4.10, we obtain:

$$u_{sup}(r, \theta, z) = \frac{w_0}{w_z} e^{-i[\alpha(r, z) - \alpha(r', 0)]} \sum_{j=1}^q e^{i\phi_j} LG_j(r', \theta, 0) \quad (4.11)$$

As we are interested in the image of the transverse section, we calculate the intensity distribution over the transverse section, product of the superposition:

$$I(r, \theta, z) = |u_{sup}(r, \theta, z)|^2 \quad (4.12)$$

$$= \left(\frac{w_0}{w_z} \right)^2 \left| \sum_{j=1}^q e^{i\phi_j(z)} LG_j(r', \theta, 0) \right|^2 \quad (4.13)$$

Since $w_0 < w_z$, $\left(\frac{w_0}{w_z} \right)^2$ always decreases through propagation.

4.3 Self image with paraxial LG beams

We call self image to the phenomenon where, while the beam is propagating through z , we recover the initial image $z = 0$ through constructive interference of the many LG beams. But what is necessary for this phenomenon to occur? Let's go back to equation 4.13. By multiplying $e^{-i\phi_1}$ to the expression inside

the vertical bars, which doesn't change the value of the intensity, we obtain:

$$I(r, \theta, z) = \left(\frac{w_0}{w_z} \right)^2 \left| \sum_{j=1}^q e^{i\Delta\phi_j(z)} LG_{p_j, l_j}(r', \theta, 0) \right|^2 \quad (4.14)$$

where $\Delta\phi_j(z) = \phi_j(z) - \phi_1(z)$.

What we are accomplishing with equation 4.14 is focusing our analysis in the relative values $\Delta\phi_j$, which makes sense as we are dealing with interference and the relative phases between the LG beams is what matters.

The intensity distribution at $z = 0$ is (4.13):

$$I(r, \theta, 0) = \left| \sum_{j=1}^q LG_{p_j, l_j}(r', \theta, 0) \right|^2 \quad (4.15)$$

where we have used the fact that $\forall j$, if $z = 0$ then $\phi_j(z) = 0$.

So, as we see from equation 4.14, the relative phases $\Delta\phi_j(z)$ are retaining us from obtaining the initial intensity distributon (4.15) of the interference of the Laguerre beams. So, the only way for us to recover the mentioned image is if the Gouy phases $\phi_j(z)$ obey the following conditions:

$$\begin{aligned} \Delta\phi_2(z) &= 2n_2\pi \\ \Delta\phi_3(z) &= 2n_3\pi \\ &\dots \\ \Delta\phi_q(z) &= 2n_q\pi \end{aligned} \quad (4.16)$$

where n 's are integer numbers greater or equal than 1, as we are supposing that the LG beam indexed with 1 (one), has the lowest order mode N , so that $\Delta\phi_j \geq 0$ will hold for all j .

What the previous equations express is a resincronization of the Gouy phases, meaning that the difference between them is a multiple of 2π which allows the constructive interference and the reappearance of the initial transverse distribution of intensity (4.15). Obviously, when the difference between the Gouy phases is not an integer multiple of 2π , we will obtain transversal configurations different from the initial one. It may not be explicit, but the condition above brings some very specific restrictions for the Gouy phases if we want *Self Image* to happen. First of all, we remember that $\Delta\phi_j(z) = \phi_j(z) - \phi_1(z) = \Delta_{N_j}\phi_0(z)$. Where we are defining the difference of mode orders $\Delta_{N_j} = N_j - N_1$ and $\phi_0(z) = \arctan(z/z_r)$. So, applying this to 4.16, we arrive at:

$$\phi_0(z) = \frac{2n_2\pi}{\Delta_{N_2}} = \frac{2n_3\pi}{\Delta_{N_3}} = \dots = \frac{2n_q\pi}{\Delta_{N_q}} \quad (4.17)$$

Then again, because of its definition, $|\phi_0| \leq \pi/2$, brings a minimum value for the mode orders differences of the LG beams:

$$\Delta_{N_j} \geq 4, \quad \forall j, \quad j = \{2, \dots, q\} \quad (4.18)$$

Because of the discrete nature of our condition (4.17), normally, self image will occur at specific distances $z = z_u$, where we are indexing with $u = \{1, \dots, S\}$, where S : total number of self images. We are gonna start counting self images from $z = 0$ until infinite. So we can rephrase condition 4.17 as:

$$\phi_0(z_u) = \frac{2n_{u,2}\pi}{\Delta_{N_2}} = \frac{2n_{u,3}\pi}{\Delta_{N_3}} = \dots = \frac{2n_{u,q}\pi}{\Delta_{N_q}} \quad (4.19)$$

$$= \frac{2n_{u,j}\pi}{\Delta_{N_j}}, \quad \forall j \quad (4.20)$$

where again, we are indexing with $u = \{1, \dots, S\}$ the number of self image we are referring to, and with $j = \{2, \dots, q\}$ the LG beam being analyzed.

This has as consequence:

$$\begin{aligned} \Delta_{N_j} &= k_j n & k_j \text{ is a positive integer} \\ n_{u,j} &= uk_j \end{aligned} \quad (4.21)$$

where n is a positive integer different from one. The equation 4.21 means that all mode order differences Δ_{N_j} need to have an integer different from one (n) as a common divisor.

Then, using 4.21 in 4.20:

$$\phi_0(z_u) = 2\pi \frac{u}{n} \quad (4.22)$$

This means “self image distances” z_u are completely determined by the self image we are referring to (u) and the common divisor n of the mode order differences Δ_{N_j} :

$$z_u = z_r \tan(2\pi u/n) \quad (4.23)$$

The number of self images S is also determined by the n :

$$S = n \setminus 4 \quad (4.24)$$

where “ \setminus ” is integer division. Notice that this self image, using interference of LG beams, is not periodic regarding the propagation coordinate z . Nevertheless we can define a parameter or variable χ which is adimensional and won't depend on the dimensions of our experiment.

$$\chi(z_u) = \frac{2}{\pi} \phi_0(z_u) = \frac{4u}{n} \quad (4.25)$$

where we have used 4.22. This parameter is limited $0 < \chi < 1$. When $z = 0 \rightarrow \chi = 0$ and when $z = \infty \rightarrow \chi = 1$. Self image is periodic regarding this parameter χ .

4.3.1 Self image with 2 LG beams

Let's consider the LG beams LG_{p_1, l_1} and LG_{p_2, l_2} .

Then, we have the condition:

$$\phi_0(z) = 2n_2\pi/\Delta_{N_2} \quad (4.26)$$

where $\Delta_{N_2} = N_2 - N_1 = 2(p_2 - p_1) + |l_2| - |l_1|$
From 4.21 and choosing $k_2 = 1$:

$$\Delta_{N_2} = n \quad n_{u,2} = u \quad (4.27)$$

The number of self images possible S is restricted by the difference of mode orders Δ_{N_2} .

$$S = \Delta_{N_2} \setminus 4 \quad (4.28)$$

where “ \setminus ” is integer division. And the self image distances (4.23):

$$z_u = z_r \tan(2\pi u/\Delta_{N_2}) \quad (4.29)$$

are completely determined by the single mode orders difference Δ_{N_2}

4.3.2 Self image with 3 LG beams

Given the 3 LG beams: LG_{p_1, l_1} , LG_{p_2, l_2} and LG_{p_3, l_3} . For self image to occur, the condition is:

$$\phi_0(z_u) = \frac{2n_{u,2}\pi}{\Delta_{N_2}} = \frac{2n_{u,3}\pi}{\Delta_{N_3}} \quad (4.30)$$

where $n_{u,2}$, $n_{u,3}$ are positive integers.

The modal order differences need to be greater or equal than 4:

$$\Delta_{N_j} \geq 4, \quad j = \{2, 3\} \quad (4.31)$$

The differences of modal orders must have a common divisor “ n ”:

$$\Delta_{N_2} = k_2 n \quad (4.32)$$

$$\Delta_{N_3} = k_3 n \quad (4.33)$$

where k_2 , k_3 are positive integers and n is a positive integer different than one.

We can predict the number of self images “ S ” by noticing that one of the k'_j s must be one. Then:

$$S = n \setminus 4 \quad (4.34)$$

where “\” is integer division.

And the self image distances will be (4.23):

$$z_u = z_r \tan(2\pi u/n) \quad (4.35)$$

4.3.3 Example

An special case is presented here, the interference of 3 LG beams with mode, radial and orbital orders:

$$\begin{aligned} LG_1 & : p_1 = 0, l_1 = 0 \rightarrow N_1 = 0 \\ LG_2 & : p_2 = 6, l_2 = 0 \rightarrow N_2 = 12 \\ LG_3 & : p_3 = 12, l_3 = 0 \rightarrow N_3 = 24 \end{aligned} \quad (4.36)$$

Notice that we have indexed the LG beams from lower to higher mode order N . So the ΔN 's are:

$$\Delta N_2 = 12 \quad \Delta N_3 = 24 \quad (4.37)$$

S the common factor is $n = 12$ and $k_2 = 1$ and $k_3 = 2$.

The number of self images S is determined by n (4.34):

$$S = 12 \setminus 4 = 3 \quad (4.38)$$

And the self image distances will be (4.23):

$$z_1 = z_r \tan(2\pi/12) \quad (4.39)$$

$$z_2 = z_r \tan(4\pi/12) \quad (4.40)$$

$$z_3 = \infty \quad (4.41)$$

We can also calculate the adimensional parameter for self images (4.25) of our example:

$$\chi_1 = 4 * 1/12 = 0.333 \quad (4.42)$$

$$\chi_2 = 4 * 2/12 = 0.666 \quad (4.43)$$

$$\chi_3 = 4 * 3/12 = 1 \quad (4.44)$$

Notice that even though self imaging is not periodic in the propagation coordinate z , it is periodic in the new parameter $\chi = \chi(z)$.

Images of the example for different distances

Using the modes of the 3 LG beams (4.36), we calculate the intensity distributions of the interference (4.14):

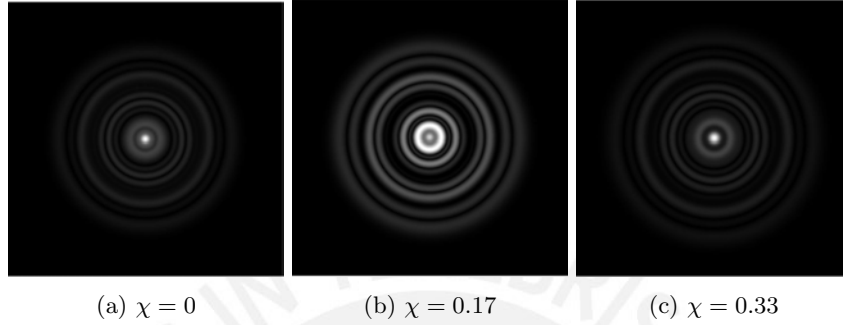


Figure 4.1: Simulation of the intensity distribution for 3 different distances z . a) is at $z = 0$. b) is in between $z = 0$ and the first self image. c) is at the first self image.

Notice that at $\chi = 0$ and at first self image ($\chi = 0.33$) the intensity is concentrated in a small circle at the center of the beam. Away from self image distances we obtain images like Fig. 4.1 b, where the intensity is more distributed towards the outer rings of the beam.

Chapter 5

Application: Concealing information using the superposition of LG beams

5.1 Using superposition of LG beams to write a word

The goal of the present work was to present an interesting application of the self image phenomenon. The application presented here is the concealing of information, with the interference of LG beams, when z is different of a self image distance z_i (4.23). So we only recover the initial image, which can be seen as revealing the information, at self image distances $z = z_i$.

We decided the initial image to be a word: UFF (Universidad Federal Fluminense). The idea is that only for self image distances $z = z_i$ we will be able to read the word. If $z \neq z_i$ we won't be able to read it. We used the 3 LG beams superposition of the previous example (4.36), as dots, to write the word UFF. In Figure 5.1 we show a simulation of the image at $z = 0$.

5.2 Spatial Light Modulator: generation of the superposition of LG beams

The SLM, for its initials Spatial Light Modulator, as its name says, modulates the phase of the incident light. The SLM has two parts. First is the screen made of pixels, where at the same time these pixels enclose a line of birefringent crystals (a line of them for each pixel). Given the amount of voltage we apply to a pixel, the corresponding line of birefringent crystals modulates the light that falls upon it. The second part of the SLM is the controller that is

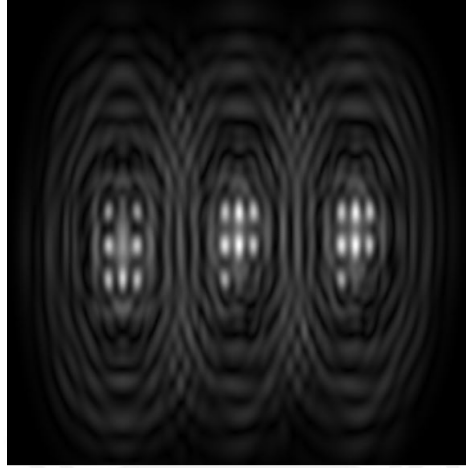


Figure 5.1: Information: the word UFF, formed up by dots which in reality are the superposition of LG beams at $z = 0$

connected to a PC. With an holographic map (picture of grays we make in the PC) we can control the voltage that we apply to each pixel. To each color of gray corresponds a voltage. From the reflection of a gaussian beam in the SLM screen, where we put the specific holographic map for the job, we obtained the desired superposition of the Laguerre beams.

The SLM used in this experiment was the PLUTO 2 model, made by Holey. It is a reflective type, with 8 bits pixels (256 gray colors) and that uses Liquid Crystal on Silicon as the birrefringent crystal. See Figure 5.2.



Figure 5.2: Spatial Light Modulator used in the experiment: PLUTO-2, Holey.

5.3 Experimental setup

Since in our analysis we supposed all Laguerre beams had the same wavelength, this parameter is not critical in the interference of the beams, we could have

used light with any wavelength available. We used a laser that provided gaussian light (in the fundamental mode) with a wavelength of $\lambda = 633nm$.

We generated the superposition of LG beams using the aforementioned SLM (Spatial Light Modulator).

We needed a bigger waist than the one obtained from the laser, for it to reach more pixels of the SLM, which makes the obtained superposition of Laguerre beams to have a better resolution. To solve this we used a telescope display (equation 3.10), which collimated the beam and augmented its waist to $800 \mu m$. We used $f_1 = 2f_2 = d_1/2 = 20cm$. See Figure 5.3

We programmed the SLM to return a superposition of beams with a waist of $w_0 = 200\mu m$. This value was optimal since the self image distances depend on the beam waist w_0 , and we had only half a meter to displace our CCD camera. This let us record until the second self image of the case we wanted to analyse (equations 4.39 and 4.40).

The SLM produces the paraxial LG beams from a diffraction grating, this also means the modulated light we are interested in exits the SLM at an specific angle from the axis of the SLM (Figure 5.3). To select only the modulated light, we first used a lens (L_3) in order to focus the light to a waist small enough that with an iris we could select only the modulated light. Here, we are left with two issues, first we have lost some centimeters of propagation of the superposition of the LG beams, and because of the L_3 lens we have a beam that is expanding. Both issues are solved with an additional lens L_4 . We use this last lens to displace the transverse section of the interference, according to equation 3.13 (notice that we need $f_3 = f_4 = d_3 = d_4/2 = d_5$). By doing this we recover the propagation of the transverse section from the beginning ($z = 0$). Also this last lens L_4 let us refocus the beam. We used $f_3 = 20cm$

With a CCD camera, and an improvised rail to displace the camera, we registered the images of the transverse section of the superposition of the beams at different positions up until $z' = 0.5m$. We decided that the best way to show the propagation of the superposition of the LG beams was via a video, so we recorded an image every 2mm. The points of major interest are the ones where we can see self images.

Self Image Setup

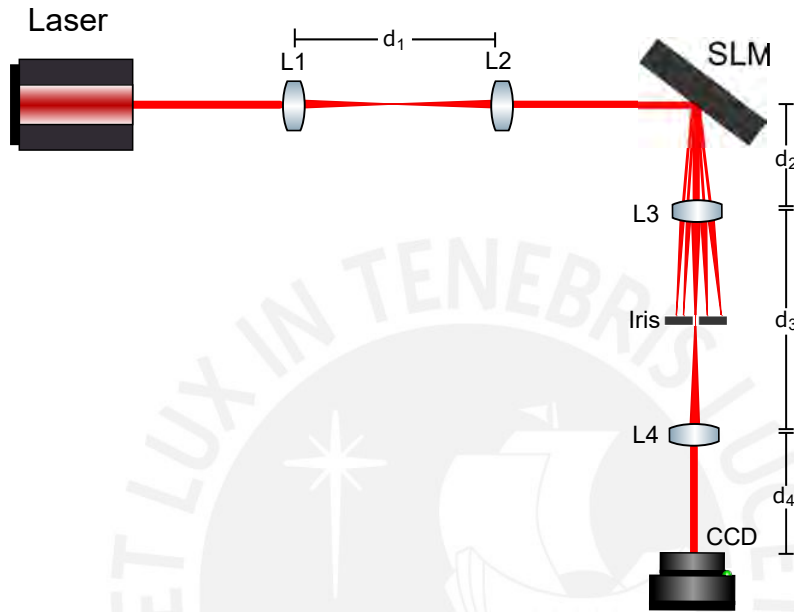


Figure 5.3: Setup

5.4 Experimental results

Using a CCD camera we registered through the propagation axis (z) the transverse section of the superposition of 3 Laguerre beams. Here we present the images at $z = 0$, first self image $z = z_1$ and second self image $z = z_2$. We also present distances in between $z = 0$ and the self images.

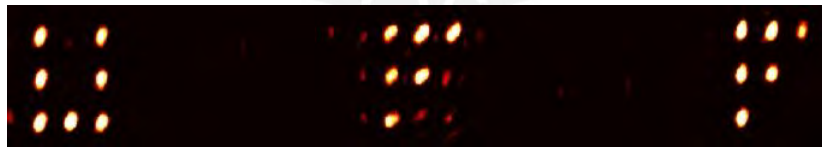


Figure 5.4: $\chi = 0$

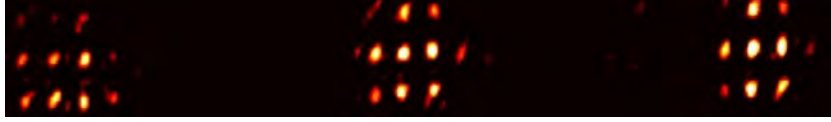


Figure 5.5: $\chi = 0.166$

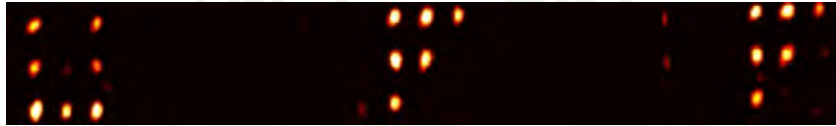


Figure 5.6: $\chi = 0.334$: 1st self image

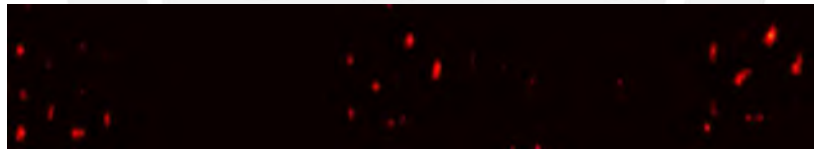


Figure 5.7: $\chi = 0.5$

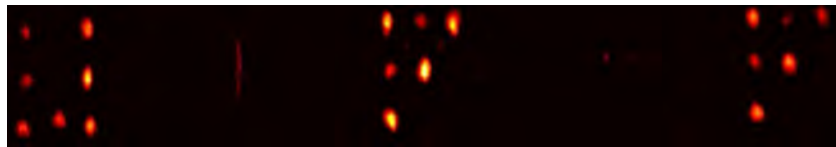


Figure 5.8: $\chi = 0.654$: 2nd self image

Chapter 6

Conclusions

In chapter 4 we calculated the behaviour of a single Laguerre beam propagating through the z coordinate (longitudinal propagation). We saw that the transverse image (intensity distribution) was an expanded version of the initial image, with the decreasing factor $\left(\frac{w_0}{w_z}\right)^2$. Then we analyzed the superposition of various coherent and collinear LG beams and showed that given a restriction on the difference of its mode orders $N = 2p + |l| + 1$, we can produce the self image phenomenon via the constructive interference of these Laguerre Gauus beams. As with a single LG beam, we discovered that the image of the superposition of LG beams expands through propagation, but with a rescaling of the radial component we can arrive at the same intensity distribution. In chapter 5 we showed an application for the self image with LG beams, we reveal information (a word) everytime self image is obtained, and we conceal the information everytime we loose the self image. We used the interference of 3 LG beams as dots to write the word. Then displacing a camera we recorded images at various distances. Self image distances were really close to the ones predicted. Experimentally, we decided to use an Spatial Light Modulator, to obtain directly from it, the interference of the 3 LG beams used in the application. We could have produced the LG beams individually and then try to interfere them, nevertheless this would have complicated the experiment unnecessarily.

The third Self image was not presented here because , at that distance, the expansion of the LG beams made the dots of the word UFF to interfere with each other, making the whole word became illegible.



Part III

PR box

Chapter 7

Introduction: PR box

Bell inequality is a very famous and successful theoretical proof of the divergence of results, between Classical (Local hidden variable theory) and Quantum Mechanics. Using this tool, over the years many experimental works have demonstrated that nature cannot be described with a local hidden variable theory. The most controversial feature of quantum mechanics: non-locality, has gain much attention over the last years because of the development of quantum information. Nowadays non-locality is widely accepted and used in many other exciting applications like teleportation, swapping, etc. Nevertheless, this opens other questions, like why is nature just as local to reach the Tsirelson's bound but not go beyond? The algebraical maximum of the CHSH inequality is 4, and quantum mechanics can only reach up to $2\sqrt{2}$. What happens in this gap that seems empty and without a theory that can describe it?

Popescu and Rhorlich proved that from non-locality and relativistic causality, quantum mechanics correlations were not the only correlations that emerged. Relativistic causality meaning that no information is transmitted with superluminal velocities. This means that there are correlations, capable of surpassing the Tsirelson's bound, that are still causal. The super-quantum correlations that maximally surpass the Tsirelson's bound, making the Bell parameter $S = 4$, are known as PR boxes in honor of Popescu and Rhorlich. In chapter 8, we review the concepts necessary to define a PR box.

Given that super-quantum correlations can't be obtained from a closed quantum ensemble, there are extra steps needed in order to obtain them. Markovitch et al, showed that, in a bipartite quantum system, adding pre and post-selection of maximally entangled states will fake the maximal surpass of the CHSH inequality. In chapter 9, we define a probability distribution of measurements in between pre and post selection of other states using the Aharonov-Bergman-Lebowitz formula.

In chapter 10 we propose an experimental setup, using spin-orbit modes of

classical light, capable of simulating a PR box.



Chapter 8

PR box: Non-locality beyond quantum mechanics

8.1 Non-locality

Once taken as negative, non-locality has become one of the most important aspects in quantum mechanics. An event here can have an effect at a very long distance, instantly. This "apparent" action at distance was the core of the critic that Einstein-Podolsky-Rosen made against quantum mechanics in their very famous paper [3]. For them, it seemed that quantum mechanics and its non-locality didn't respect relativistic causality.

For quantum mechanics to violate relativistic causality, there would need to be an exchange of messages between parties faster than light. Uncertainty makes the outcome of a measurement to be probabilistic, this makes impossible to transmit messages using non-locality. The correlations between the distant particles are blurry enough for a message not to be send. So nowadays, we say that no-determinism (uncertainty) makes it possible for non-locality and relativistic causality to coexist.

8.2 Entanglement and Non-locality

Though, entanglement and non-locality are related, it is now widely accepted that they are two different concepts.

Entanglement refers to the impossibility of separating a bipartite state as a product of 2 functions, where each one contain information about only one of the parties.

$$|\psi\rangle \neq |\psi_1\rangle \otimes |\psi_2\rangle \quad (8.1)$$

Non-locality is the possibility of correlation between very distant objects given that they share a common past. Using the Bell theorem, we say that if

Bell parameter results greater than 2, there is non-locality.

$$|S| > 2 \quad (8.2)$$

The relation between these two definitions is very well known for closed bipartite systems. Non-entangled systems give a Bell parameter equal to 2, and maximally entangled states (or Bell states) give the maximum violation of Bell inequalities $2\sqrt{2}$.

8.3 CHSH inequality

Bell inequalities are a powerful tool to witness non-locality. The CHSH inequality is derived from the Bell's, but it has a more convenient structure for the experimental work. Therefore is by non-offical concensus one of the more used Bell type of inequalities. CHSH inequalities refer to experiments involving two parties very distant from each other (analogue to two independet degrees of freedom), in such a way that they are out of each other's light cone. As usual let's refer to these parties as Alice and Bob.

Let's suppose we give each of them a particle. These two particles share a common past in such a way that we can say that now, they are correlated. We define a quantity named correlation C_{AB} as average values of the observables (A for Alice and B for Bob) measured by each party. We are dealing with two-possibility variables or bits, our measured values can be $+1$ or -1 .

The correlations are expressed as:

$$\begin{aligned} C_{AB} &= \langle AB \rangle \\ &= p(+1, +1|A, B) + p(-1, -1|A, B) - p(+1, -1|A, B) - p(-1, +1|A, B) \end{aligned} \quad (8.3)$$

where $p(\alpha, \beta|A, B)$ is the joint probability of measuring α if A was measured by Alice and β if B was measured by Bob. $\alpha, \beta = \{+1, -1\}$ are the possible outcomes of each measurement for Alice and Bob respectively.

With the correlations, we define the Bell parameter:

$$S = C_{AB} + C_{A'B} + C_{AB'} - C_{A'B'} \quad (8.5)$$

where A' and B' are other arbitrary bases.

Using a local hidden variable theory, it can be shown that the predicted Bell parameter in the CHSH structure is constrained by 2:

$$|S_{clas}| < 2 \quad (8.6)$$

In the same way, Quantum Mechanic's predicted Bell parameter has 2 as it lower constraint.

Tsirelson [4] demonstrated that Quantum Mechanics also had an upper limit value of $2\sqrt{2}$ for the Bell parameter .

$$2 < |S_{qm}| \leq 2\sqrt{2} \quad (8.7)$$

8.4 Axioms of Quantum Mechanics

Why is quantum mechanics limited by $2\sqrt{2}$ in the CHSH inequality? One can say that mathematically it is because of the Hilbert structure. Popescu and Rhorlich [5] suspected that it expressed a limit imposed by the relativistic causality. Although they were wrong, this led them into an interesting result.

Under the suggestion of Aharonov, Popescu and Rhorlich questioned the axioms attributed to quantum mechanics. These axioms were widely agreed to be uncertainty and relativistic causality. And non-locality was seen as a consequence of the "axioms" mentioned above. If non-locality and relativistic causality are taken as axioms, will quantum mechanics be the only theory that emerges? Popescu and Rhorlich discovered that the answer was: No. This new superquantum correlations violated Bell inequalities, they also could surpass the Tsirelson's bound, even achieving the maximum algebraic value 4. All this, respecting the relativistic causality.

Super-quantum correlations still obey relativistic causality, the difference with quantum correlations is that they are "more" non local. Unfortunately, the universe is not only causal and non-local. Even if this two axioms capture the essence of the beauty of quantum mechanics, the lack of a mathematical theory to, from a description of our physical reality, arrive to this super-quantum correlations forces us to place them in an imaginary situation too far away from our reality.

8.5 Black Box

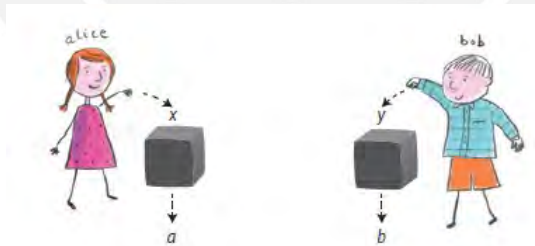


Figure 8.1: Black box

Since what we are going to analyze is a theory outside the classical or quantum realm, we need to avoid their formalism and stick to a very general definition of Bell inequalities. This can be achieved by using a black box as the space where Alice and Bob do their respective experiments.

Our black box takes bits as inputs from each party, bit x for Alice and bit y for Bob ; and returns bits as outputs to each party, bit a for Alice and bit b

for Bob. We don't know what happens inside the box. The information we can extract from experiments Alice and Bob do with their respective bits is contained in the probability distribution $p(ab|xy)$. This is a conditional probability that can be read as: "the probability of Alice obtaining the bit a and Bob obtaining the bit b , given that Alice introduced the bit x and Bob the bit y ". This probabilities satisfy the non negativity condition:

$$p(ab|xy) \geq 0, \quad \forall a, b, x, y \quad (8.8)$$

And the normalization condition:

$$\sum_{a,b} p(ab|xy) = 1, \quad \forall x, y \quad (8.9)$$

Another condition is that there can't be signaling between both parties. This means that one parties output can't depend on the other's input. This is known as the no-signaling condition. Since we are dealing with very distant parties, signaling will mean relativistic causality violation.

Mathematically the no-signaling condition for Alice, can be expressed as:

$$\sum_b p(a, b|x, y) = \sum_b p(a, b|x, y') = p(a|x) \quad \forall a, x, y, y' \quad (8.10)$$

And for Bob:

$$\sum_a p(a, b|x, y) = \sum_a p(a, b|x', y) = p(b|y) \quad \forall b, y, x, x' \quad (8.11)$$

8.6 CHSH inequality: revisited

Now that we have defined another formalism for Bell tests, we rewrite the equations for correlations and Bell Factor.

The analogy between the Bell tests and these black boxes experiments is that in both we are dealing with bits: two-possibility variables. In the Bell tests, Alice and Bob select the observable of measurement (A or A' for Alice and B or B' for Bob). This can be seen in the black box as Alice and Bob selecting the input bit 0 or 1. Also, in the Bell tests they obtain an outcome (α for Alice and β for Bob) that can have 2 values $+1$ or -1 , which is the same as in the black box where Alice and Bob obtain an output bit 0 or 1.

So, the analogy is:

$$p(ab|xy) \equiv p(\alpha, \beta|A, B) \quad (8.12)$$

The input bits x and y take the place of the observables A and B , and the output bits a and b replace the outcomes α and β .

This derives in re-expressing the correlations:

$$C_{xy} = p(00|xy) + p(11|xy) - p(01|xy) - p(10|xy) \quad (8.13)$$

and the Bell factor as:

$$S = C_{11} + C_{01} + C_{10} - C_{00} \quad (8.14)$$

8.7 PR box

Superquantum correlations appear when we take non-locality and relativistic causality as axioms. We call PR box to the super-quantum correlations that surpass maximally the Tsirelson's bound ($S = 4$). To define the PR box we can depart from the black box definition. So a PR box is a black box that has an additional condition [6]:

$$x.y = a \oplus b \quad (8.15)$$

where “.” is multiplication and “ \oplus ” is known as addition modulo 2:

\oplus	0	1
0	0	1
1	1	0

This means that when $x.y = 1$ (which happens when $x = y = 1$), a and b can only be different. And for all the other cases $x.y = 0$, a and b can only have the same value. Also let us suppose that all possibilities are equiprobable. So the probability distribution $p(ab|xy)$ is:

Input $(x, y) \setminus$ Output (a, b)	00	01	10	11
00	1/2	0	0	1/2
01	1/2	0	0	1/2
10	1/2	0	0	1/2
11	0	1/2	1/2	0

Table 8.1: Probability distribution $p(ab|xy)$

8.8 CHSH inequality: PR box

With the values of the conditional probabilities in Table 1, we construct the correlations:

$$C_{00} = p(00|00) + p(00|11) - p(00|01) - p(00|10) = 1/2 + 1/2 - 0 - 0 = 1 \quad (8.16)$$

The same way goes for the other correlations, yielding in:

$$C_{01} = C_{10} = 1 \quad C_{11} = -1 \quad (8.17)$$

So, the Bell parameter will be:

$$S_{PR\ box} = 4 \quad (8.18)$$

8.9 PR-boxes in Communication Complexity

It has been shown that if PR-boxes were real, they could help solve many nowaday problems [7]. One of these possible applications concerns the amount of bits required for the communication between two parties. There is a very useful function in Theory of Communication, named the AND function.

We can use an example to illustrate the unbelievable consequences of PR-boxes. Alice and Bob are friends distant from each other, and want to meet some day of the year. To make the connection with the AND function, let us suppose that what they want to know is if the number of days when they can meet is an odd or an even number. If we denote x (y) the bit of information for Alice (Bob), where this bit encodes the information of availability of each party. The mentioned bit is 0 if the person is busy that day, and 1 if the person is free. Using this notation, what they want to know is if $\sum_i x_i y_i$ is even or odd. The problem is that this value requires that at least one person has access to the bits of the other party in order to calculate the summation and see if the number is odd or even. In 2012, Wim van Dam [8], using the results from his PHD thesis showed that using a PR box the above problem (which is known as Inner Product function) could be simplified.

If PR-boxes were physically realizable, Alice and Bob's laboratories could be a black box and they could use the x_i and y_i as input bits for experiments yielding in a_i and b_i as outcome bits. So using the PR-box definition, we would have:

$$x_i y_i = a_i \oplus b_i \quad \forall i \quad (8.19)$$

So the quantity we want to know if is even or odd can be re-expressed in terms of the output bits a and b .

$$\sum_i x_i y_i = \sum_i a_i \oplus b_i = \sum_i a_i \oplus \sum_i b_i \quad (8.20)$$

Notice, we don't know anything from the experiments that were made in each laboratory to yield the output bits. We only know that the correlation, between them and the input bits, is governed by the condition 1 of the PR boxes.

As stated in the previous equation, addition modulo 2 is also separable in summation, so the value of interest is separated in 2 bit values $\sum_i a_i$ and $\sum_i b_i$. The summation is made with addition modulo 2. This has the advantage that Alice can calculate $\sum_i a_i$ by her own, same goes for Bob with $\sum_i b_i$. It is necessary

to remark that a_i and b_i are outcome bits obtained via experiments ruled by super quantum correlations between the mentioned bits. Then Bob can send its bit (0 if $\sum_i b_i$ is even, or 1 if it's odd) to Alice, and Alice with her own bit (0 if $\sum_i a_i$ is even, or 1 if it's odd) can determine if $\sum_i x_i y_i$ is even or odd. As shown in the last paragraph Bob has to send only 1 bit to Alice for her to determine if the value $\sum_i x_i y_i$ is even or odd. This contrast with the raw case of Bob having to send his 365 bits y_i (one for each day of the year) to Alice, and then her to determine if the value of interest $\sum_i x_i y_i$ is even or odd. What is even more surprising is that 365 is a number that arrived because of the nature of the example we gave, it could have actually been any number and the PR-box would still reduce it to only 1.



Chapter 9

Simulation of a PR-box using a Quantum Mechanics ensemble

Super quantum correlations can't be obtained directly from the Bell test in a closed quantum mechanics ensemble. All the same, it was first showed by Cabelo et al. [10] that, via the post-selection of two qubits out of a tri-partite maximally entangled state (GHZ state), that we could simulate correlations that maximally surpassed Tsirelson's bound. An experimental work using this approach was done by Chen et al. [11] using the polarization of three single photons to form up a GHZ state. Another method, which is the one we use in the experimental proposal of this work, involves pre and post-selection of bipartite entangled states from a bipartite state. To describe the process we will use the Aharonov-Bergman-Lebowitz formula, which yields the probability of a possible outcome, given that there is pre and post-selection of states. Additionally we need to evaluate what states are pre and post-selected, they have respect the no-signaling condition and also be able to replicate the probability distribution of a PR box (Table 8.1). The observables to be measured are also important and we need to select them accordingly.

9.1 Measurements in Quantum Mechanics

In quantum mechanics, we can't predict the outcome of the measurement on a system $|\psi_i\rangle$, we can only express the probability of each possible outcome. Let C be the observable of the measurement, c_j one of the eigenvalues and $|c_j\rangle$ the respective eigenvector. Then, the conditional probability of the outcome c_j , given that initially the system is described by $|\psi_i\rangle$ is:

$$p(c_j|\psi_i) = |\langle c_j|\psi_i\rangle|^2 \quad (9.1)$$

9.2 The Aharonov-Bergman-Lebowitz formula

Let us assume that we have knowledge of the quantum system in two different moments: $|\psi_i\rangle$ and $|\psi_f\rangle$, and we want to know the probability of a measurement in between this two states.

The mathematical approach for this has been demonstrated for non-degenerated [12] and degenerated [13] states. The probability of a measurement of the observable C giving the value c_n between two other measurements, that yield $|\psi_i\rangle$ and $|\psi_f\rangle$, is:

$$p(c_j|\psi_i, \psi_f) = \frac{|\langle\psi_f|P_{c_j}|\psi_i\rangle|^2}{\sum_n |\langle\psi_f|P_{c_n}|\psi_i\rangle|^2} \quad (9.2)$$

where P_{c_j} is the projection operator of the measurement of C that gives the outcome c_j . The way to arrive to the previous equation is to consider the probability as the joint probability of obtaining the middle state $|c_j\rangle$ from $|\psi_i\rangle$ and of obtaining the state $|\psi_f\rangle$ from the middle state $|c_j\rangle$.

Until now, we have assigned values of 0 or 1 to our bits. We did that because it helped describe the PR box condition 8.15. But experimentally, they don't provide any insight. From now on, until we say otherwise, we will use the spin notation.

In a Bell test context, Alice and Bob, manipulate a projector in each respective laboratory. First, we need to define the observable. For the measurement of observable A , given that the 2 eigenvalues are $+1$ or -1 , we can define 2 projectors :

$$P_{A=+} \quad \text{outcome} : +1 \quad (9.3)$$

$$P_{A=-} \quad \text{outcome} : -1 \quad (9.4)$$

We can connect the Black box's input values $x = \{0, 1\}$ and $y = \{0, 1\}$ with the observables $x = \{A, A'\}$ and $y = \{B, B'\}$ that are controlled by Alice and Bob in a Bell test. In the same way, the Black box's outputs $a = \{0, 1\}$ and $b = \{0, 1\}$, will be the possible eigenvalues $a = b = \{+, -\} \equiv \{\uparrow, \downarrow\}$ which are the outcomes of a measurement in the Bell test.

Our interest in bipartite states takes us to express the projector of measurement as a tensorial product of 2 projectors, each one of a different vectorial space (Alice or Bob). In Alice's vector space the possible bases of measurement are represented by x and the possible outcomes of the measurement as a , so $P_{(x=a)}$ is the projector in Alice's vector space for the outcome a in the base of measurement x . Similarly goes for Bob's vector space with y and b . So, using the definitions from the previous paragraph, we define the ABL formula with the bits x, y, a, b , and the initial and final states ($|\psi_i\rangle$ and $\langle\psi_f|$):

$$p(a, b|x, y, |\psi_i\rangle, \langle\psi_f|) = p(a, b|x, y) = \frac{|\langle\psi_f|P_{x=a} \otimes P_{y=b}|\psi_i\rangle|^2}{\sum_{a', b'} |\langle\psi_f|P_{x=a'} \otimes P_{y=b'}|\psi_i\rangle|^2} \quad (9.5)$$

Since we are gonna use the same initial and final quantum states for all the simulation ($|\psi_i\rangle$ and $\langle\psi_f|$), we can remove them from the notation of the probabilities, but keeping in mind that these are still dependent on those states. Nonetheless, this still doesn't simulate a PR box. We need a probability distribution as in Table 8.1. To accomplish this, we need specific pre and post selected states $|\psi_i\rangle$ and $|\psi_f\rangle$, and observables x, y .

9.3 With what quantum pre and post selected states can we simulate a PR box?

No-signaling

Markovitch et al showed which combination of pre and post-selected ensembles will make the probabilities (9.2) simulate the ones of a PR box [9]. Let's start by saying that there are 3 groups which satisfy no-signalling condition (eq. 8.10):

- Separable states (non-entangled)

$$|\psi_i\rangle = |\uparrow\uparrow'\rangle \quad (9.6)$$

$$|\psi_f\rangle = |\uparrow''\uparrow'''\rangle \quad (9.7)$$

The disadvantage of this states is that, since they are not entangled, they don't exhibit non-locality, so they won't be useful.

- Maximally entangled states (Bell states):

$$|\psi_i\rangle = \frac{1}{\sqrt{2}}(|\uparrow\uparrow'\rangle + e^{i\theta_i}|\downarrow\downarrow'\rangle) \quad (9.8)$$

$$|\psi_f\rangle = \frac{1}{\sqrt{2}}(|\uparrow''\uparrow'''\rangle + e^{i\theta_f}|\downarrow''\downarrow'''\rangle) \quad (9.9)$$

- Same states, just with their amplitudes swapped:

$$|\psi_i\rangle = \alpha|\uparrow\uparrow'\rangle + e^{i\theta}\beta|\downarrow\downarrow'\rangle \quad (9.10)$$

$$|\psi_f\rangle = \beta|\uparrow\uparrow'\rangle + e^{-i\theta}\alpha|\downarrow\downarrow'\rangle \quad (9.11)$$

Maximal surpass of the Tsirelson's bound

Nevertheless, the swapped states can't achieve the maximal surpass of the Tsirelson's bound, so they are of no use in our simulation. That is why we decided to use a pair of Bell states as initial and final states:

$$|\psi_i\rangle = \frac{1}{\sqrt{2}}(|\uparrow_z\uparrow_z\rangle + |\downarrow_z\downarrow_z\rangle) \quad (9.12)$$

$$\langle\psi_f| = \frac{1}{\sqrt{2}}(\langle\uparrow_z\uparrow_x| - \langle\downarrow_z\downarrow_x|) \quad (9.13)$$

In the same way, this doesn't work for every choice of base of measurement. For this corresponding initial and final states (9.12 and 9.13), we chose the basis of measurement:

$$x = \{\sigma_x, \sigma_z\}, \quad y = \{\sigma_z, \sigma_x\} \quad (9.14)$$

With our pre and post-selected states (9.12, 9.13) and observables (9.14), we construct probabilities following the ABL formula (9.5). This yields in the following probability distribution $p(a, b|x, y, |\psi_i\rangle, \langle\psi_f|) = p(a, b|x, y)$:

Input $(x, y) \setminus$ Output (a, b)	$\uparrow\uparrow$	$\uparrow\downarrow$	$\downarrow\uparrow$	$\downarrow\downarrow$
(σ_x, σ_z)	1/2	0	0	1/2
(σ_x, σ_x)	1/2	0	0	1/2
(σ_z, σ_z)	1/2	0	0	1/2
(σ_z, σ_x)	0	1/2	1/2	0

Table 9.1: Probability distribution $p(ab|xy, \psi_i, \psi_f)$

Table 9.1 is the same as Table 8.1, this gives us certainty that we will have super-quantum correlations.

$$C_{\sigma_x, \sigma_z} = C_{\sigma_x, \sigma_x} = C_{\sigma_z, \sigma_z} = 1, \quad C_{\sigma_z, \sigma_x} = -1 \quad (9.15)$$

Resulting in a Bell parameter which maximally surpass the Tsirelson's bound:

$$S = 4 \quad (9.16)$$

Chapter 10

Experimental Proposal to simulate a PR-box using polarization and transverse mode spaces

10.1 Polarization and transverse mode as vector spaces

In the previous chapter we showed a way to simulate a PR box using a bipartite system. We used the spin notation, but obviously it works for any analogous vector space.

We can use polarization and transverse mode (First order Hermite-Gauss modes) as the 2 vector spaces. This type of light modes are also known as spin-orbit modes [14]. An arbitrary vector of spin-orbit light mode can be written as:

$$\vec{E} = c_1 HG_{1,0}(\vec{r}) \hat{e}_H + c_2 HG_{1,0}(\vec{r}) \hat{e}_V + c_3 HG_{0,1}(\vec{r}) \hat{e}_H + c_4 HG_{0,1}(\vec{r}) \hat{e}_V \quad (10.1)$$

where the c 's are complex numbers satisfying the normalization condition ($|c_1|^2 + |c_2|^2 + |c_3|^2 + |c_4|^2 = 1$). And $HG_{1,0}$ ($HG_{0,1}$) is the horizontal (vertical) transverse mode (equation 1.16); \hat{e}_H (\hat{e}_V) is the horizontal (vertical) polarization.

Although entanglement is one of the fundamental features of Quantum Mechanics, it has been shown over the years that Maxwell or classical fields can exhibit a similar feature that is sometimes called non-separability to differentiate it. We can even describe the degrees of freedom of the classical fields with the same mathematics of the qbits.

So we can represent our spin-orbit mode using the quantum notation [14]:

$$|\psi\rangle = c_1 |H\rangle \otimes |h\rangle + c_2 |H\rangle \otimes |v\rangle + c_3 |V\rangle \otimes |h\rangle + c_4 |V\rangle \otimes |v\rangle \quad (10.2)$$

where $|H\rangle$ ($|V\rangle$) represents the horizontal (vertical) polarization. And $|h\rangle$ ($|v\rangle$) is the horizontal (vertical) transverse mode.

The following table shows the notation we are gonna use for the projectors, on each vector space and its analogy with the spin notation:

Projector	spin	polarization	TM
$P_{\sigma_z=\uparrow}$	$ \uparrow_z\rangle \langle\uparrow_z $	$ H\rangle \langle H $	$ h\rangle \langle h $
$P_{\sigma_x=\uparrow}$	$ \uparrow_x\rangle \langle\uparrow_x $	$ D\rangle \langle D $	$ d\rangle \langle d $
$P_{\sigma_z=\downarrow}$	$ \downarrow_z\rangle \langle\downarrow_z $	$ V\rangle \langle V $	$ v\rangle \langle v $
$P_{\sigma_x=\downarrow}$	$ \downarrow_x\rangle \langle\downarrow_x $	$ A\rangle \langle A $	$ a\rangle \langle a $

where $|D\rangle = \frac{1}{\sqrt{2}}(|H\rangle + |V\rangle)$
where $|A\rangle = \frac{1}{\sqrt{2}}(|H\rangle - |V\rangle)$

Table 10.1: Analogy between vector spaces

10.2 Local Unitary Operations

A local unitary operation can be represented as a Jones matrix [15]:

$$U(\hat{n}, \gamma) = \cos(\gamma/2) \mathbb{1} - i \sin(\gamma/2) \hat{n} \cdot \vec{\sigma} \quad (10.3)$$

where $\hat{n} = (n_x, n_y, n_z)$ is a unitary vector composed by real numbers, and $\vec{\sigma} = (\sigma_x, \sigma_y, \sigma_z)$ is a vector composed by the Pauli matrices. So $\hat{n} \cdot \vec{\sigma} = n_x \sigma_x + n_y \sigma_y + n_z \sigma_z$.

Bloch sphere

The previous definition (10.3) makes a lot of sense when we use the Bloch (or Poincaré) sphere to graph our state (in one DOF) via the Stokes parameters. Given an initial single q-bit state $|\psi\rangle$, we apply an unitary operation $U(\hat{n}, \gamma)$. In the sphere, the unitary operation rotates the state (vector) around the rotation axis given by the unitary vector \hat{n} , and γ will be the rotation angle.

For example, if the rotation axis is $\hat{n} = \hat{k}$ and the rotation angle $\gamma = \pi$, the rotation, in the sphere, looks like in figure 10.1.

10.2.1 Local Unitary operators in polarization space

In polarization DOF (or space), experimentally, we can apply unitary operators using as birrefringent waveplates. This elements have the propertie of dephasing orthogonal polarizations that incide in their rapid and slow optical axis.

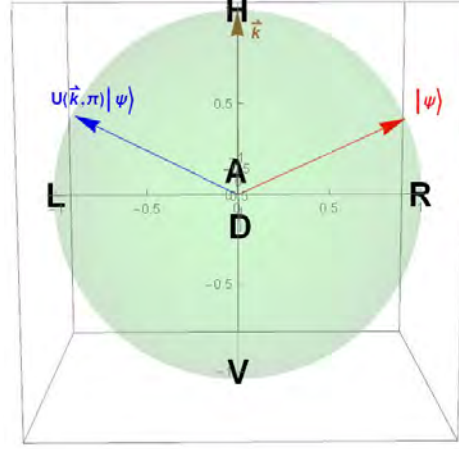


Figure 10.1: Example of the rotation due to a local unitary operation, over a single q-bit state $|\psi\rangle$, with parameters $\hat{n} = \hat{k}$ and $\gamma = \pi$.

The most common are the half wave plate (HWP or simply H) and the quarter wave plate (QWP or Q). The names given refer to the amount of dephasing they do to the orthogonal polarizations that incide on them. You can even rotate this waveplates to give more complexity to the operation. The Jones' matrix representation of these elements is as follows:

$$H(\theta) = U(\hat{n}', \pi) = -i \begin{pmatrix} \cos 2\theta & \sin 2\theta \\ \sin 2\theta & -\cos 2\theta \end{pmatrix} \quad (10.4)$$

$$Q(\theta) = U(\hat{n}', \pi/2) = \frac{1}{\sqrt{2}} \begin{pmatrix} 1 - i \cos 2\theta & -i \sin 2\theta \\ -i \sin 2\theta & 1 + i \cos 2\theta \end{pmatrix} \quad (10.5)$$

where θ is rotation angle of each waveplate, and $\hat{n}' = (\sin 2\theta, 0, \cos 2\theta)$.

In general, the type of operations done by the half and quarter waveplates (equations 10.4 and 10.5) are known as π mode converter and $\pi/2$ mode converter respectively. They receive these names because of the angle they rotate the state in the Bloch sphere. They also can be fulfilled by optical elements in the transverse-mode space.

10.2.2 Local Unitary operators in transverse-mode space

As in polarization DOF, in transverse-mode DOF we can arrange optical elements that act as π mode converter and $\pi/2$ mode converter. A Dove prism inverts the transmitted image and, when rotated θ , rotates the image twice: 2θ . Eventhough the image is rotated, the polarization is not [16]. So, the Dove prisms (DP) acts as a π mode converter in the transverse mode DOF. For the $\pi/2$ mode converter you can use two identical cylindrical lenses of focal length

f , distanced by $\sqrt{2}f$ [17].

$$DP(\theta) = U(\hat{n}', \pi) = -i \begin{pmatrix} \cos 2\theta & \sin 2\theta \\ \sin 2\theta & -\cos 2\theta \end{pmatrix} \quad (10.6)$$

$$MC_{\pi/2}(\theta) = U(\hat{n}', \pi/2) = \frac{1}{\sqrt{2}} \begin{pmatrix} 1 - i \cos 2\theta & -i \sin 2\theta \\ -i \sin 2\theta & 1 + i \cos 2\theta \end{pmatrix} \quad (10.7)$$

where again θ is the angle of rotation, of the optical element, from its optical axis and $\hat{n}' = (\sin 2\theta, 0, \cos 2\theta)$

10.3 Projectors

Given a closed system, a projector is defined due to an observable $A = \hat{n}_A \vec{\sigma}$, with eigenvalues $|c_i\rangle$ and its respective possible outcome c_i . So the observable A can be decomposed in its spectral decomposition: $A = \sum_i c_i P_{A=c_i}$, where $P_{A=c_i}$ is the projector due to the measurement of the observable A and the outcome c_i . Also because of completeness, $\sum_i P_{A=c_i} = \mathbb{1}$.

Given that our states are q-bits, we call $\{|+\rangle, |-\rangle\}$ to the eigenvalues of A and $+1, -1$ to the respective possible outcomes. So the previous equations become:

$$A = P_{A=+} - P_{A=-} \quad (10.8)$$

$$\mathbb{1} = P_{A=+} + P_{A=-} \quad (10.9)$$

So, the projectors are defined as:

$$P_{A=\pm} = \frac{1}{2}(\mathbb{1} \pm A) = \frac{1}{2}(\mathbb{1} \pm \hat{n}_A \cdot \vec{\sigma}) \quad (10.10)$$

Experimentally we have arrangements of optical elements capable of doing projections in both spaces.

10.3.1 Polarizing beam splitter

In polarization DOF we have an optical element called polarization beam splitter (PBS), this are used to split polarized light into 2 paths. The PBS produce a separation of 90° between the output beams. It transmits light with polarization parallel to the optical axis of the PBS, and reflects light with polarization perpendicular to its axis. This definition, is represented by the following projections:

$$\begin{aligned} |H\rangle \langle H| & , & \text{if we take the transmission path} & \quad (10.11) \\ |V\rangle \langle V| & , & \text{if we take the reflexion path} \end{aligned}$$

Nevertheless this is too limited, a more general projection can be achieved, selecting the transmission path, and putting the PBS in between 2 half wave plates rotated the same angle (Figure 10.2):

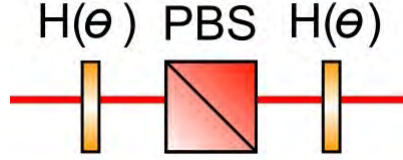


Figure 10.2: PBS+2HWPs form up a projector of the linear polarization $|\theta\rangle$.

$$U_{pbs}(\theta) = H(\theta) |H\rangle \langle H| H(\theta) \quad (10.12)$$

$$U_{pbs}(\theta) = |\theta\rangle \langle \theta| \quad (10.13)$$

where $|\theta\rangle = H(\theta) |H\rangle = \cos(2\theta) |H\rangle + \sin(2\theta) |V\rangle$

This would be enough for the type of projections necessary in this work, as we can see from the observables to be used in equation 9.14.

Alternately, to project linear polarization we can also use an optical element known as polarizer. A rotation θ from its optical axis is represented in Jones matrix:

$$P(\theta) = |\theta\rangle \langle \theta| \quad (10.14)$$

which is the same as our PBS + 2HWPS setup (Figure 10.2).

10.3.2 Transverse-mode beam splitter

A transverse-mode beam splitter (TMBS) is feasible using a Mach-Zhender interferometer with an additional mirror and a Half-wave plate in one arm (MZIM + HWP)[18].

The idea here is that, in the polarization DOF, a reflection produces a phase-shift of π only in the horizontal polarization $|H\rangle$. In the same way, in the transverse-mode DOF, a reflection produces a phaseshift of π only on the horizontal Hermite-Gauss $|h\rangle$. This means that the bipartite state $|Hh\rangle$ will gain a phase π twice, resulting in no phase gained; the same goes for $|Vv\rangle$ which doesn't gain any phase at all. Both $|Hv\rangle$ and $|Vh\rangle$ gain a π phase.

In summary, in a reflection, our bipartite states (polarization \otimes transverse-

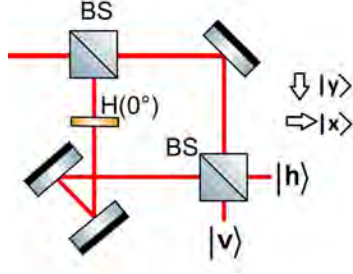


Figure 10.3: TMBS. Given light coming from the $|x\rangle$ path, the transmitted path will have transverse state $|h\rangle$ ($HG_{1,0}$) and the reflected path will have $|v\rangle$ ($HG_{0,1}$).

mode space) will gain phases as:

$$\begin{aligned}
 |Hh\rangle &\longrightarrow e^{i2\pi} |Hh\rangle = |Hh\rangle \\
 |Vv\rangle &\longrightarrow e^{i0\pi} |Vv\rangle = |Vv\rangle \\
 |Hv\rangle &\longrightarrow e^{i\pi} |Hv\rangle = -|Hv\rangle \\
 |Vh\rangle &\longrightarrow e^{i\pi} |Vh\rangle = -|Vh\rangle
 \end{aligned} \tag{10.15}$$

Additionally, a half wave plate at 0° adds a π phase to horizontal polarization $|H\rangle$ compared to vertical polarization $|V\rangle$. So if we consider a $H(0^\circ)$ and a reflection, we will have the following phases:

$$\begin{aligned}
 |Hh\rangle &\longrightarrow e^{i\pi} |Hh\rangle = -|Hh\rangle \\
 |Vv\rangle &\longrightarrow e^{i0\pi} |Vv\rangle = |Vv\rangle \\
 |Hv\rangle &\longrightarrow e^{i2\pi} |Hv\rangle = |Hv\rangle \\
 |Vh\rangle &\longrightarrow e^{i\pi} |Vh\rangle = -|Vh\rangle
 \end{aligned} \tag{10.16}$$

The transformation in 10.16 can be expressed in Jones matrix or kets representation as:

$$\begin{aligned}
 U_p &= \begin{pmatrix} -1 & 0 & 0 & 0 \\ 0 & 1 & 0 & 0 \\ 0 & 0 & 1 & 0 \\ 0 & 0 & 0 & -1 \end{pmatrix}_{pol \otimes tm} \\
 &= |Hh\rangle e^{i\pi} \langle Hh| + |Vh\rangle e^{i\pi} \langle Vh| + |Hv\rangle \langle Hv| + |Vv\rangle \langle Vv| \tag{10.18}
 \end{aligned} \tag{10.17}$$

As we can see, after passing through the $H(0)$ and the reflection, $|Hh\rangle$ and $|Vh\rangle$ have the same π phase, and $|Hv\rangle$ and $|Vv\rangle$ have the same null phase. This difference in phases of the states is what makes possible the separation of the orthogonal transverse modes $|h\rangle$ and $|v\rangle$ in the TMBS.

Using the Jones' matrix representation of the various optical elements used (Annex 15.1), and considering the path vector space $\{|x\rangle, |y\rangle\}$ where x is the

horizontal path and y the vertical path, we are going to calculate the Jones matrix of the whole Transverse-mode beam splitter, Figure 10.3.

We are going to use the path DOF as an ancilla. The objective will be that, similar to a PBS, light with horizontal Hermite-Gauss mode $|h\rangle$ continues by the same path and light with vertical Hermite-Gauss mode $|v\rangle$ changes path.

As we see in Figure 10.3, first we have a BS, followed by a conditional operation inside the Mach Zehnder, this conditional operation applies U_p (10.16) to light in the $|y\rangle$ path and a phaseshift $e^{i\phi}$, that can be adjusted using a piezoelectric in the mirror, to the path $|x\rangle$ with respect to the path $|y\rangle$. We choose the dephasing to be $\phi = -\pi/2$. After this, comes a second BS. All this is summarized in the ket representation of the whole transformation (see Annex 13.1):

$$U_{tmbs} = U_{bs}.U_{mirr}.(\mathbb{1}_{4x4} \otimes |x\rangle e^{-i\pi/2} \langle x| + U_p \otimes |y\rangle \langle y|).U_{bs} \quad (10.19)$$

$$= \begin{pmatrix} 1 & 0 & 0 & 0 & 0 & 0 & 0 & 0 \\ 0 & 1 & 0 & 0 & 0 & 0 & 0 & 0 \\ 0 & 0 & 0 & i & 0 & 0 & 0 & 0 \\ 0 & 0 & -i & 0 & 0 & 0 & 0 & 0 \\ 0 & 0 & 0 & 0 & 1 & 0 & 0 & 0 \\ 0 & 0 & 0 & 0 & 0 & 1 & 0 & 0 \\ 0 & 0 & 0 & 0 & 0 & 0 & 0 & i \\ 0 & 0 & 0 & 0 & 0 & 0 & -i & 0 \end{pmatrix}_{pol \otimes tm \otimes path} \quad (10.20)$$

$$= \mathbb{1}_{pol} \otimes |h\rangle \langle h| \otimes \mathbb{1}_{path} + \mathbb{1}_{pol} \otimes |v\rangle e^{i\pi/2} \langle v| \otimes (|x\rangle \langle y| - |y\rangle \langle x|)$$

This means that if the light entering has horizontal Hermite Gauss mode $|h\rangle$, it exits the TMBS without any change of polarization, transverse-mode or path, only with an additional phase of π . On the contrary, if the light has vertical Hermite Gauss mode $|v\rangle$, it would only change its path, with an additional phase π if the light came from the path $|x\rangle$.

If light enters only from the $|x\rangle$ path, and at the end we select only the light of the $|x\rangle$ path, we have the transformation ($pol \otimes tm$):

$$U_{tmbs-h} = \langle x| U_{tmbs} |x\rangle = \mathbb{1}_{pol} \otimes |h\rangle \langle h| \quad (10.21)$$

More general projector

Same as in polarization space, in transverse mode space we can make a projector that projects linear combinations of $|h\rangle$ and $|v\rangle$. (Figure 10.4)

Given that light comes in through from the $|x\rangle$ path, if at the end we select only the light going to the $|x\rangle$ path, and sandwich the TBMS with 2 Dove prisms with the same rotation angle, we will have:

$$\begin{aligned} U_{tmbs}(\theta) &= DP(\theta) |h\rangle \langle h| DP(\theta) \\ &= |g\rangle \langle g| \end{aligned} \quad (10.22)$$

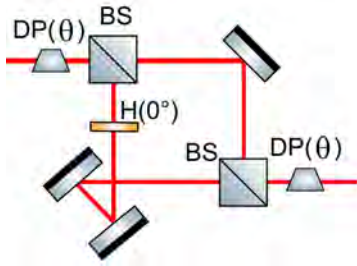


Figure 10.4: MZIM + HWP(0) in one arm form up a TMBS. If we sandwich the transmission path with 2 Dove prisms we obtain a more general projector.

where $|g\rangle = DP(\theta) |h\rangle = \cos(2\theta) |h\rangle + \sin(2\theta) |v\rangle$

10.4 Stages to simulate a PR box

As stated before, the simulation consists in 3 stages: pre-selection, projective measurements and post-selection.

Pre-selection	Measurements (projections)	Post-selection
$ \psi_i\rangle$	$(P_{x=a} \otimes P_{y=b}) \psi_i\rangle$	$\langle\psi_f (P_{x=a} \otimes P_{y=b}) \psi_i\rangle$

Table 10.2: We need 3 stages to simulate the PR-box. In this table we sketch what happens with the quantum state over the 3 stages. First, the pre-selection of the state $|\psi_i\rangle$. Secondly, the local-projections in the x and y observables that give the a and b outcomes respectively. Thirdly, we select only states in the final state $|\psi_f\rangle$.

As we see in Table 10.2, after the post-selection stage, the probability of outcomes, $x = a$ (Alice measuring the x observable and obtaining a) and $y = b$ (Bob measuring the y observable and obtaining b) is proportional to:

$$p(a, b|x, y, \psi_i, \psi_f) \propto |\langle\psi_f| (P_{x=a} \otimes P_{y=b}) |\psi_i\rangle|^2 \quad (10.23)$$

Normalizing the previous equation 10.23, we obtain the ABL formula (equation 9.5).

10.5 Proposed Experimental Setup

There have already been experimental quantum displays capable of simulating a PR box [11] [19] and even with classical light [20].

What we propose here (Figure 10.5) is a very simple display that uses polarization and transverse mode of a beam of classical light. The pre-selection made by a single optical element (S-plate), projective measurements are done with polarizers. The post-selection is made by a CNOT (with polarization as control and transverse mode as target) composed by 2 PBDs and a Dove prism rotated 45° , a Transverse-Mode beam splitter (feasible with a Mach-Zhender interferometer with an additional mirror and a HWP in one arm), and a PBS .

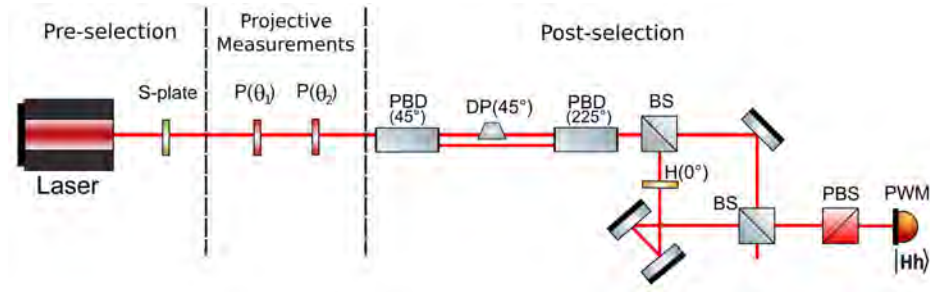


Figure 10.5: Complete setup for the simulation of a PR box, using polarization and transversal mode as degrees of freedom in classical light. P: polarizer, PBD: polarizing beam displacer, DP: Dove prism, BS: Beam splitter, H: half wave plate, PBS: polarizing beam splitter, PWM: powermeter

10.5.1 Pre-selection

S-plate

The pre-selection is done by an S-plate, that transforms linear polarization into radial polarization (Figure 10.6 and equation 10.25).

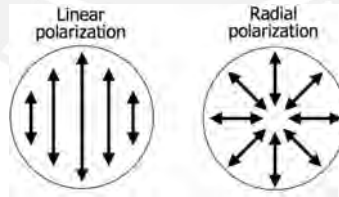


Figure 10.6: In a bipartite state, linear polarization is represented by a separable state, while radial polarization, by the entangled state in equation 10.25

The Jones matrix of the S-plate is:

$$M_{s-plate} = |\psi\rangle_{radial} \langle H| + |\psi\rangle_{azim} \langle V| \quad (10.24)$$

where $|\psi\rangle_{radial} = \frac{1}{\sqrt{2}}(|Hh\rangle + |Vv\rangle)$ and $|\psi\rangle_{azim} = \frac{1}{\sqrt{2}}(|Hh\rangle - |Vv\rangle)$.

Using the S-plate we can select the initial state. The method is to align the S-plate optical axis with the horizontal polarization. This allows us, given that the light coming from the laser is polarized horizontally $|H\rangle$, we obtain the desired pre-selected state $|\psi_i\rangle$, which is also called radial vector beam:

$$|\psi_i\rangle = |\psi\rangle_{radial} = \frac{1}{2}(|Hh\rangle + |Vv\rangle) \quad (10.25)$$

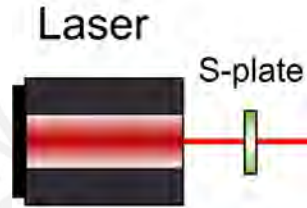


Figure 10.7: A laser emitting horizontal polarization and an S-plate are enough to pre-select the initial state $|\psi_i\rangle$

10.5.2 Projective Measurements

The Bell test is designed for Alice and Bob to do projective measurements in each respective laboratory. Nonetheless, because we are dealing with maximally entangled states (Bell states), Alice could do the projection that corresponds to Bob in her own laboratory (see Annex 13.2 and 13.3)

To do the projective measurement in the transverse mode, the usual procedure would be to use TBM (transverse mode beam splitter) and a pair of Dove prisms (10.22). The combination of this optical elements would harden the experimental procedure, because they would use an interferometer, that in addition with the one in the post-selection, can difficult the control of the relative phases. Also, the Dove prisms, rotated in angles different from 0° or 45° , induce small changes in polarization that would lead to different results from the ones we anticipate.

Having this in mind, we propose doing both projections in the polarization DOF, this saves us from having to use the TMBS and the 2 Dove prisms mentioned in the above paragraph. But let's remember that this is possible because the state over which we are going to make the projections is maximally entangled (MES or Bell state). We propose using a pair of polarizers, the first one to project on the transverse mode DOF and the second to project on the polarization DOF. See Figure 10.8

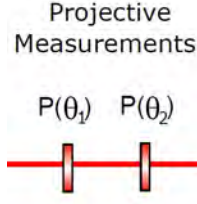


Figure 10.8: The projective measurements are made with a pair of polarizers, with θ_1 we control the projection in transverse mode DOF and with θ_2 we control the projection of the polarization DOF

For the projections corresponding to the transverse mode, the procedure is as follows:

<i>Spin projection</i>	<i>Ket projection</i>	θ_1
$(P_{\sigma_z=\uparrow})_{tm}$	$ h\rangle\langle h $	0^0
$(P_{\sigma_z=\downarrow})_{tm}$	$ v\rangle\langle v $	45^0
$(P_{\sigma_x=\uparrow})_{tm}$	$ d\rangle\langle d $	22.5^0
$(P_{\sigma_x=\downarrow})_{tm}$	$ a\rangle\langle a $	-22.5^0

Table 10.3: Values of the angle θ_1 to accomplish the different projections corresponding to the transverse mode DOF.

In the same way, and more obviously, for the projection corresponding to the polarization DOF:

<i>Spin projection</i>	<i>Ket projection</i>	θ_2
$(P_{\sigma_z=\uparrow})_{pol}$	$ H\rangle\langle H $	0^0
$(P_{\sigma_z=\downarrow})_{pol}$	$ V\rangle\langle V $	45^0
$(P_{\sigma_x=\uparrow})_{pol}$	$ D\rangle\langle D $	22.5^0
$(P_{\sigma_x=\downarrow})_{pol}$	$ A\rangle\langle A $	-22.5^0

Table 10.4: Values of the angles θ_2 to accomplish the different projections corresponding to the polarization DOF.

From the different possible combinations of angles θ_1 and θ_2 (Table 10.3 and 10.4), we can make the 16 possible projections, necessary to calculate the Bell parameter:

$$(P_{x=a})_{pol} \otimes (P_{y=b})_{tm} \quad (10.26)$$

10.5.3 Post-selection

This step is aimed at post-selecting the final state $|\psi_f\rangle = \frac{1}{\sqrt{2}}(|Dv\rangle + |Ah\rangle)$. Notice that this is an entangled state, so its post-selection requires a non-local type of operation. The post-selection has 2 parts: a CNOT gate and the selection of the separable state $|Hh\rangle$. See figure 10.9

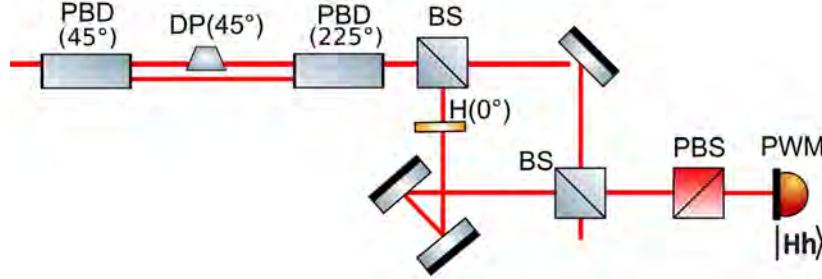


Figure 10.9: Setup that does the post-selection of the final state $\langle\psi_f|$

C-NOT

A controlled-not operation (C-NOT), in a bipartite state, applies a $\sigma_x = \begin{pmatrix} 0 & 1 \\ 1 & 0 \end{pmatrix}$ (known as NOT operation) over the target if the control DOF is in the state $|1\rangle$ and the identity operation if the control DOF is in the state $|0\rangle$. The 4x4 matrix and the ket representation of the CNOT are:

$$CNOT = \begin{pmatrix} 1 & 0 & 0 & 0 \\ 0 & 1 & 0 & 0 \\ 0 & 0 & 0 & 1 \\ 0 & 0 & 1 & 0 \end{pmatrix} \quad (10.27)$$

$$= |0\rangle\langle 0|_{control} \otimes \mathbb{1}_{target} + |1\rangle\langle 1|_{control} \otimes (\sigma_z)_{target} \quad (10.28)$$

In our display, we want to use polarization as the control and transverse mode as the target. Mathematically, represented in the kets notation, in our bipartite system, the operation we want the C-NOT to perform is:

$$CNOT = |D\rangle\langle D| \otimes \sigma_x + |A\rangle\langle A| \otimes \mathbb{1} \quad (10.29)$$

For this purpose we propose the use of a Polarizing Beam Displacer (PBD), and not the usual Mach-Zhender setup (10.10) because we already have an interferometer (MZIMs with half wave plate) in the complete setup (Figure

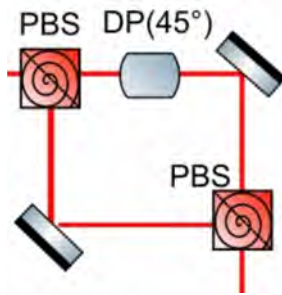


Figure 10.10: A Mach-Zehnder interferometer and a Dove prism in one arm, form up a CNOT with polarization as control and transverse mode as target.

10.5) and a second one would be detrimental for the stabilization of the relative phases in the paths.

Figure 10.10 shows an alternitavely way of doing the CNOT, the twisted lines in the PBS tell us that these are letting $|D\rangle$ polarization transmit and they reflect the $|A\rangle$ polarization. This can be done rotating the PBS by 45° , or by puting a HWP at 22.5° before the first PBS and after the second PBS.

Polarizing Beam Displacer (PBD)

A polarizing beam displacer (PBD) is a birrefringent optical element that separates orthogonal polarizations of an incident light, like a PBS. The difference is that a PBS separates them in paths making a 90° angle, but the PBD separates them in collinear paths, a couple of centimeters away from each other. Just like any other birrefringent element, when rotated, we can change the polarizations that are separated.

If the optical axis of the PBD is parallel to the horizontal plane of our experiment table, the PBD is going to transmit horizontal polarization (without any change). But it will displace vertical polarization a few centimeters (this distance depends on the manufacturing details), this displacement also adds a relative phase to vertical polarization, because of the path travelled due to the displacement. See figure 10.11

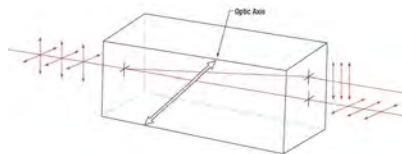


Figure 10.11: PBD with its optical axis paralel to horizontal polarization. It lets $|H\rangle$ pass, and displaces $|V\rangle$.

CNOT using PBDs

The initial PBD@45, rotated 45°, will transmit, without displacing it, diagonal polarization, but the antidiagonal polarization $|A\rangle$ will be displaced towards the down level. A second PBD@225, rotated 225°, will displace the light with antidiagonal polarization towards the up level, and won't do anything to $|D\rangle$ polarization. So we can use the first PBD to separate the polarizations, then place a Dove prism at 45°, which operates as the first Pauli matrix in the transverse mode space, to the diagonal polarization level. Finally the second PBD recombines both levels into a single path beam. All this is again resumed by the desired C-NOT operation (equation 10.29).



Figure 10.12: CNOT, with polarization as control and transverse mode as target, using a pair of PBDs.

We can summarize the C-NOT effect over a bipartite state, by showing the effect over the orthogonal base in which we are going to do the post-selection:

$$|\psi_f\rangle = \frac{1}{\sqrt{2}}(|Dv\rangle + |Ah\rangle) \xrightarrow{CNOT} |Hh\rangle \quad (10.30)$$

$$\text{States we want to avoid } \begin{cases} \frac{1}{\sqrt{2}}(|Dh\rangle + |Av\rangle) \xrightarrow{CNOT} |Hv\rangle \\ \frac{1}{\sqrt{2}}(|Dv\rangle - |Ah\rangle) \xrightarrow{CNOT} |Vh\rangle \\ \frac{1}{\sqrt{2}}(|Dh\rangle - |Av\rangle) \xrightarrow{CNOT} |Vv\rangle \end{cases}$$

So our problem of post-selecting $\langle\psi_f|$ from the other states of its basis, has transformed into the post-selection of the separable state $\langle Hh|$ from the other separable states of the basis it composes.

Selection of the $\langle Hh|$ state

To complete our post-selection process, we need to post-select $\langle Hh|$, for this purpose we use a PBS and a TMBS, the combination of both optical elements let us separate spatially the 4 states of the separable orthonormal basis: $\{|Hh\rangle, |Hv\rangle, |Vh\rangle, |Vv\rangle\}$. We measure light's intensity, with a powermeter (PWM), only on the $|Hh\rangle$ path, and loose the light of the other paths. See figure 10.13. This concludes the post-selection process.

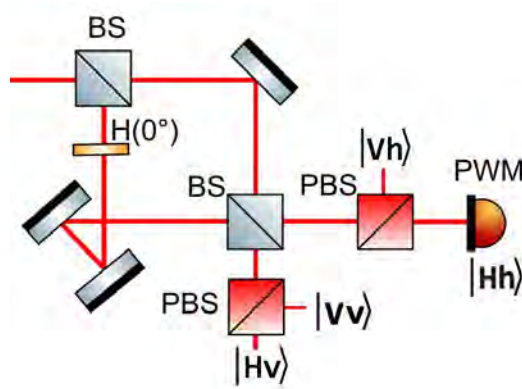


Figure 10.13: TMBS+PBS. Using path as an ancilla, we obtain the state $\langle Hh|$ in one of the 4 exit paths.

CNOT + TMBS + PBS

The whole post-selection setup (combination of CNOT+TMBS+PBS) yields in the following transformation:

$$\begin{aligned}
 POSTSELECT &= |Hh\rangle \langle Hh| . CNOT \\
 &= |Hh\rangle \langle Hh| (|D\rangle \langle D| \otimes \sigma_x + |A\rangle \langle A| \otimes \mathbb{1}) \quad (10.31) \\
 &= |Hh\rangle \langle \psi_f|
 \end{aligned}$$

This transformation takes light only if it is in the state $|\psi_f\rangle$ (and filtrates it from its orthogonal states). Even though, it disentangles the bipartite state, it gives us the corresponding intensity (probability) of the $|\psi_f\rangle$ state.

10.5.4 Measurement of the probability distribution

Now, gathering the 3 steps, pre-selection, projection and post-selection, at the powermeter we will have an intensity proportional to:

$$I_{Hh}(a, b, x, y) \sim ||Hh\rangle \langle \psi_f| P_{x=a} \otimes P_{y=b} |\psi_i\rangle|^2 = p(a, b|x, y) \quad (10.32)$$

So the probability distribution will be measured as:

$$p(a, b|x, y) = \frac{I_{Hh}(a, b, x, y)}{\sum_{a', b'=\uparrow, \downarrow} I_{Hh}(a', b', x, y)} \quad (10.33)$$

where the possible values of the observables are $x = \{\sigma_x, \sigma_z\}$ and $y = \{\sigma_z, \sigma_x\}$. And the angles for the polarizers θ_1 and θ_2 that do the projections are in Table 10.3 and 10.4.

Chapter 11

Discussions

11.1 PR boxes make bits share too much information

If Alice and Bob could use the non-local correlations to exchange super-luminal information, this will mean that if they choose an input bit, they would know with certainty what the other party will obtain as an output bit (notice the input bit for the last party doesn't matter). Alice and Bob can't use their bits to communicate with each other. If they did, this will mean that nature wasn't respecting relativistic causality.

Nevertheless, PR boxes exhibit what can be called super correlations, or correlations more non local than their quantum counterparts. This derives not in super-luminal information exchange; but in extra-information being shared between the correlated parts. For example Alice, knowing her input and output bit, can guess with utter certainty something about Bob's output. To be more precise with what this "something" means, we can analyse as follows:

- If Alice chooses $x = 0$ as her input bit, given what bit a she obtains from her experiment, she knows what bit Bob will obtain, it doesn't matter what Bob chose as his input y . More specifically here the something Alice knows is that $b = a$. This can be seen in the condition 1 of the PR box. If $x = 0$; the multiplication xy is always 0, it doesn't matter the value of y and b is always the same as a . Obviously this also holds true the other way around, from the Bob's point of view.
- If Alice chooses $x = 1$ as her input bit, given what bit a she obtains, she knows the dependence of Bob's output on his input bit. More specifically, if $a = 0$ then $b = y$ and if $a = 1$ then $b = y \oplus 1$.

11.2 Loopholes in Bell inequalities

Loopholes had already been used in the past to fake or simulate violations of Bell inequalities [21]. In the same way, we have showed that they can be used to fake a maximal violation of them.

Specifically, detection loophole has been used in many ways. For example, forcing a dynamic variation of the source for the Bell test, this means that depending on the probability you want to measure, you alter the state of the source. This can be seen as a dynamic pre-selection for faking a Bell violation. Other case is a post-selection, which is a selection after the change of basis, but before the projections of the state to be measured. Finally the case we have used, which is a post-selection after the measurement process, which goes more hand in hand with the Black box formalism because we are doing the "additional step" after the Black box.

11.3 Opinion on the application of PR-boxes in Communication Complexity

We have showed an interesting possible application of PR-boxes in a real problem (section 10.9). Also we showed that PR-boxes can be simulated using a quantum mechanics ensemble by the exploit of loopholes (section 12.5). So what stops us from using this simulation on a real world problem to take advantage of the benefits of PR-boxes?

Let's talk specifically about the Communication Complexity application we presented here and the simulation we proposed (pre and post selection of a bipartite quantum ensemble). There are 2 type of loopholes we exploit when simulating a PR-box as we proposed. The first one is the detection loophole, when doing a post-selection of a quantum state, we are favouring the detection of one quantum state over the others. If the desired post-selected state was separable, we would only need to use the detection loophole. Post-selection would take place in each laboratory and a PR-box would be simulated. Unfortunately, Markotvitch [9] showed that in order to simulate PR-boxes using post-selection, the pre and post-selected states must be maximally entangled states. Because of this, we need to make a Bell measurement, which means distinguish a Bell state over the other 3 orthogonal Bell states. As showed, this is feasible with a non-local operation. For this purpose, in our proposed setup, we added a CNOT gate that functions as a dis-entangling operation. This yields in the exploit of a locality loophole between Alice and Bob, because CNOT gate is a conditional type of operation, meaning that the result of one party will depend on the input of the other, which also doesn't follow the no-signalling condition of a PR box.

Chapter 12

Conclusions

In chapter 8 we reviewed the concept of the Bell type inequality: CHSH, and its connection with a Black Box, which helped us define a PR box, name for the superquantum correlations capable of surpassing the Tsirelson's bound.

In chapter 9 we presented the ABL formula, which helped us define the probability distribution of a quantum ensemble capable of simulating a PR box. We also chose the quantum states to be pre and post selected, and the observables to be measured by Alice and Bob, that will be used for the simulation.

In chapter 10 we described some optical elements necessary for the experimental simulation of a PR box, using spin-orbital laser modes of light. Then we showed an experimental setup, consisting of 3 parts. First, pre-selection of a maximally entangled state $|\psi_i\rangle$ using an S-plate. Then, instead of doing projections in each DOF, we proposed doing both projections on the polarization degree of freedom, using 2 polarizers at different angles. Finally, we showed how to post-select the maximally entangled state $|\psi_f\rangle$, using a CNOT (polarization as control, and transverse mode as target) which disentangles the state to be selected and transforms it into $|Hh\rangle$, then a Transverse mode beam splitter (TMBS) followed by a polarizing beam splitter (PBS) that are capable of post-selecting $|Hh\rangle$. By moving the polarizers of the projection part, we can obtain the 16 necessary projections. We showed that by measuring the intensity on each combination, at the end of our setup, we can construct the probability distribution capable of simulating a PR box.

Chapter 13

Annex

13.1 Jones matrix representation in the tripartite space

13.1.1 Half wave plate's

A half wave plate $H(\theta)$, which is rotated θ from its axis, only acts on the polarization space:

$$U_h(\theta) = \begin{pmatrix} \cos 2\theta & \sin 2\theta \\ \sin 2\theta & -\cos 2\theta \end{pmatrix}_{pol} \otimes \mathbb{1}_{tm} \otimes \mathbb{1}_{path} \quad (13.1)$$

13.1.2 Mirror's

Since we consider the path $|x\rangle$ as the horizontal and $|y\rangle$ as the vertical, the reflection (by mirrors) on the corners of the MZIM, change the path to the opposite. This can be represented with the first Pauli Matrix σ_x :

$$U_{mirr} = \mathbb{1}_{pol} \otimes \mathbb{1}_{tm} \otimes (\sigma_x)_{path} \quad (13.2)$$

13.1.3 Beam Splitter's

Ideally, Beam Splitters don't change polarization nor transverse mode of an incident beam. But they add phases depending of where did the beam come and in which direction it is exiting.

$$U_{bs} = \mathbb{1}_{pol} \otimes \mathbb{1}_{tm} \otimes \frac{1}{\sqrt{2}} \begin{pmatrix} 1 & i \\ i & 1 \end{pmatrix}_{path} \quad (13.3)$$

13.2 Local unitary operations in a Bell state

Sometimes as an experimentalist, in a bipartite system, you don't have access to every local-unitary operation in one of the DOF's (Alice's). But when we are

dealing with maximally entangled states (or Bell states) we can use the other DOF (Bob's) to apply a local-unitary operation (LUO) equivalent to an specific LUO in the aforementioned DOF (Alice's).

This can be seen as:

$$U_A(\hat{n}_1, \gamma_1) \otimes \mathbb{1}_B |\psi\rangle \equiv \mathbb{1}_A \otimes U_B(\hat{n}_2, \gamma_2) |\psi\rangle \quad (13.4)$$

where the subindexes tell us in which DOF the operator is being applied. And $\hat{n}_a = (n_{a1}, n_{a2}, n_{a3})$, $\hat{n}_b = (n_{b1}, n_{b2}, n_{b3})$,

It can be shown that for any bipartite quantum state $|\psi\rangle$, the unique solution for equation 13.4 is $U_A = U_B = \mathbb{1}$.

Nevertheless, for specific states, like the Bell states, it can be shown that we can have local unitary operations in both DOFs that have an equivalent effects over the aforementioned states.

Our state of interest being, $|\psi^+\rangle = (|Hh\rangle + |Vv\rangle)\sqrt{2}$. It can be shown that the equivalence 13.4 holds for $\gamma_a = \gamma_b$ and $\hat{n}_a = \hat{n}_b$ only if $n_{a2} = n_{b2} = 0$:

$$U_A(\hat{n}_a, \gamma_a) \otimes \mathbb{1}_B |\psi^+\rangle = \begin{pmatrix} \cos(\gamma_a/2) - in_{a3} \sin(\gamma_a/2) \\ (-in_{a1} - n_{a2}) \sin(\gamma_a/2) \\ (-in_{a1} + n_{a2}) \sin(\gamma_a/2) \\ \cos(\gamma_a/2) + in_{a3} \sin(\gamma_a/2) \end{pmatrix} \quad (13.5)$$

$$\mathbb{1}_A \otimes U_B(\hat{n}_b, \gamma_b) |\psi^+\rangle = \begin{pmatrix} \cos(\gamma_b/2) - in_{b3} \sin(\gamma_b/2) \\ (-in_{b1} + n_{b2}) \sin(\gamma_b/2) \\ (-in_{b1} - n_{b2}) \sin(\gamma_b/2) \\ \cos(\gamma_b/2) + in_{b3} \sin(\gamma_b/2) \end{pmatrix} \quad (13.6)$$

If we compare both results (13.5 and 13.6), they coincide when:

$$n_{b1} = n_{a1}, \quad n_{b2} = -n_{a2}, \quad n_{b3} = n_{a3} \quad (13.7)$$

In other words, given that we have the Bell state $|\psi^+\rangle$, we can apply the LUO in Alice's space $U_A(n_{a1}, n_{a2}, n_{a3}, \gamma_a)$ and have the same result that if we applied a similar LUO $U_B(n_{a1}, -n_{a2}, n_{a3}, \gamma_a)$ but in the other DOF.

But, if we have operations with $n_2 = 0$, the LUO's in both DOF's is the same.

$$U_A(\hat{n}, \gamma) \otimes \mathbb{1}_B |\psi^+\rangle = \mathbb{1}_A \otimes U_B(\hat{n}, \gamma) |\psi^+\rangle, \quad \hat{n} = (n_1, 0, n_3) \quad (13.8)$$

For the other Bell states ($|\psi^-\rangle, |\phi^+\rangle, |\phi^-\rangle$), it can be shown that LUO's parameters (\hat{n}, γ) need to obey different conditions, than $|\psi^+\rangle$, in order to obtain the equivalence 13.4.

13.3 Projections in a Bell state

Just like with local operators, we can show that a projection by Alice can have the same effect over the bipartite state as a projection by Bob. Given that the aforementioned state is a MES. For our purpose, the state is $|\psi^+\rangle$

$$P_{A=\pm} \otimes \mathbb{1} |\psi^+\rangle = \mathbb{1} \otimes P_{B=\pm} |\psi^+\rangle$$
$$\frac{1}{2} \begin{pmatrix} 1 + n_{a3} \\ n_{a1} - in_{a2} \\ n_{a1} + in_{a2} \\ 1 - n_{a3} \end{pmatrix} = \frac{1}{2} \begin{pmatrix} 1 + n_{b3} \\ n_{b1} + in_{b2} \\ n_{b1} - in_{b2} \\ 1 - n_{b3} \end{pmatrix} \quad (13.9)$$

The solution is that given the values for the projector in Alice's space $\hat{n}_a = (n_{a1}, n_{a2}, n_{a3})$, Bob's values will be:

$$n_{b1} = n_{a1}, \quad n_{b2} = -n_{a2}, \quad n_{b3} = n_{a3} \quad (13.10)$$

A special case is when the observable is a combination of σ_1 and σ_3 , so $n_{a2} = n_{b2} = 0$. Then $A = B$ will satisfy 13.9.

Bibliography

- [1] David L Andrews and Mohamed Babiker, *The angular momentum of light*, Cambridge University Press (2012).
- [2] Orazio Svelto, *Principles of Lasers*, Springer, Fifth Edition (2010).
- [3] Einstein, A.; Podolsky, B.; Rosen, N. (1935). "Can Quantum-Mechanical Description of Physical Reality Be Considered Complete?". *Physical Review* 47: 777-780.
- [4] B. S. Cirel'son, Quantum Generalizations of Bell's Inequality, *Lett. Math. Phys.* 4, 93 (1980).
- [5] Popescu, S. & Rohrlich, D. Quantum nonlocality as an axiom. *Found. Phys.* 24, 379 (1994).
- [6] Barrett, J., and S. Pironio," Popescu-Rohrlich Correlations as a Unit of Nonlocality", *Phys. Rev. Lett.* 95, 140401 (2005).
- [7] S. Popescu, "Nonlocality beyond Quantum Mechanics", *Nat. Phys.* 10, 264 (2014).
- [8] Dam, W. van. Implausible Consequences of Superstrong Nonlocality. *Nat. Comput.* 12, 9 (2013).
- [9] Marcovitch, S., Reznik, B. & Vaidman, L. Quantum-mechanical realization of a Popescu-Rohrlich box. *Phys. Rev. A* 75, 022102 (2007).
- [10] Cabello, A. Violating Bell's Inequality Beyond Cirel'son's Bound. *Phys. Rev. Lett.* 88, 060403 (2002).
- [11] Chen, Y. A. et al. Experimental Violation of Bell's Inequality beyond Tsirelson's Bound. *Phys. Rev. Lett.* 97, 170408 (2006).
- [12] Aharonov, Yakir and Bergmann, Peter G. and Lebowitz, Joel L. "Time Symmetry in the Quantum Process of Measurement". *Phys. Rev.* 134.B 1410 (1964)
- [13] Aharonov, Y. & Vaidman, L. Complete description of a quantum system at a given time. *J. Phys. A: Math. Gen.* 24, 2315 (1991).

- [14] M. Passos, W. Balthazar, J. A. de Barros, C. Souza, A. Khoury, and J. Huguenin, Classical analog of quantum contextuality in spin-orbit laser modes, *Phys. Rev. A* 98, 062116 (2018).
- [15] Nielsen, M. & Chuang, I., *Quantum Computation and Quantum Information*, Cambridge University Press (2000)
- [16] Padgett, M. & Paul L. Dove prisms and polarized light, *Journal of Modern Optics*, 46:2, 175 (1999)
- [17] Beijerbergen, M. et al. Astigmatic laser mode converters and transfer of orbital angular momentum, *Opt. Commun.* 96, 123 (1993).
- [18] Sasada, H., and M. Okamoto, "Transverse-mode beam splitter of a light beam and its application to quantum cryptography", *Phys. Rev. A* 68, 012323 (2003).
- [19] Tasca, D. S., Walborn, S. P., Toscano, F. & Souto Ribeiro, P. H. Observation of tunable Popescu-Rohrlich correlations through postselection of a Gaussian state. *Phys. Rev. A* 80, 030101 (2009).
- [20] N. Sandeau, H. Akhouayri, A. Matzkin, and T. Durt, Experimental violation of Tsirelson's bound by Maxwell fields, *Phys. Rev. A* 93, 053829 (2016).
- [21] Gerhardt, I. et al. Experimentally faking the violation of bell's inequalities. *Phys. Rev. Lett.* 107, 170404 (2011).